UNIVERSITY OF CALIFORNIA
SANTA CRUZ

DISSOLVED SCANDIUM AND IRON IN THE OCEAN: AN INVESTIGATION INTO THE POTENTIAL USE OF SCANDIUM DISTRIBUTIONS AND INTO A NEW REGION OF IRON LIMITATION

A dissertation submitted in partial satisfaction
of the requirements for the degree of

DOCTOR OF PHILOSOPHY

in

OCEAN SCIENCES

by

Claire E. Parker

March 2016

The dissertation of Claire E. Parker is approved:

_____
Professor Kenneth W. Bruland, Chair

_____
Professor A. Russell Flegal

_____
Professor Raphael M. Kudela

_____
Professor Christopher A. Edwards

_____
Tyrus Miller
Vice Provost and Dean of Graduate Studies

TABLE OF CONTENTS

List of Tables and Figures

CHAPTER 3: IRON LIMITATION OFF THE OREGON COAST

Abstract

DISSOLVED SCANDIUM AND IRON IN THE OCEAN:
AN INVESTIGATION INTO THE POTENTIAL USE OF SCANDIUM
DISTRIBUTIONS AND INTO A NEW REGION OF IRON LIMITATION
by
Claire E. Parker

The objective of this dissertation was to expand upon the very different states of knowledge of dissolved scandium (Sc) and iron (Fe) in the ocean. Iron is highly-studied and important biologically as an essential and often limiting micronutrient, yet characterizing the cycling of Fe fully has proved challenging. Scandium, in contrast, has barely been studied in the ocean prior to this dissertation, yet upon investigation reveals potentially useful attributes including the possibility of shedding some light on the oceanic Fe cycle. The first chapter of this dissertation characterizes the distribution and reactivity of dissolved Sc by comparing deep-water Atlantic to Pacific concentration ratios of Sc with other, better characterized Group IIIA and IIIB trivalent metals: yttrium (Y), lanthanum (La), gallium (Ga), and aluminum (Al). Results indicate that Sc is a hybrid-type metal, more particle reactive than Y and La in Group IIIB and less particle reactive than Ga and Al in Group IIIA, with an inferred oceanic residence time on the order of 1000 years. Results also suggest that Sc may represent the non-nutrient side of the oceanic Fe cycle. Chapter 2 investigates the potential to use the particle reactivity difference between Sc and its periodic table group-mates Y and La to give an indication of scavenging intensity. Results indicate that Sc, Y and La are input to the surface North Atlantic Ocean in relatively constant ratios compared with the dissolved ratios, suggesting that the variations in the

dissolved ratios are due to Sc removal through scavenging. Dissolved Y/Sc and La/Sc ratios correlate well with the shape of the gyre, suggesting that they may be driven by and provide indication of export production. Chapter 3 brings the story back to Fe with an investigation of Fe-limitation of coastal diatoms off the coast of southern Oregon. There are many studies demonstrating Fe-limitation off the California coast, but so far the Oregon coastline had only been shown to have elevated Fe from the Columbia River. Results from Chapter 3 provide evidence for Fe-limitation of growth rate and biomass accumulation of coastal diatoms off the southern Oregon coast near Cape Blanco, indicating that the Fe-limitation mosaic extends further north than previously known.

Acknowledgements

It is my pleasure to thank the many people who have contributed to the work in this dissertation and my positive experience as a graduate student. First, my advisor Ken Bruland has been fantastic. He is always willing and enthusiastic to talk about science, always supportive of my goals, always willing to offer advice, and always ready to share his excitement. It has been a great pleasure to work with Ken, and I hope that the large pile of our data that did not make it into this dissertation ensures that we continue to work together for some time. Second, Geo Smith has been consistently supportive, both with phenomenal advice on analytical methods, on which I have heavily relied, and with his enduring confidence in my ability to figure out the current problem. I would also like to thank my committee members (Russ Flegal, Raphe Kudela, and Chris Edwards) for their help with this dissertation and throughout my graduate school career. Rob Franks has my endless gratitude for his patient and expert assistance with instrumental analysis and for his willingness to help with any problem I come up with. Dondra Biller has been a huge help throughout my graduate student career by demonstrating analytical methods, explaining satellite imagery code, giving tips for smooth exams, and always being willing to offer graduate school advice. My friend Blaise Thompson has always been ready to discuss figures, data processing, and other aspects of graduate school life, for which I am very grateful. The "Woodshop Guys," Steve Ornellas, Dan Frisch, and Rob Antrobus, have been ever helpful and I have always enjoyed cheery and positive encounters with them (which so often occurred when one of them would come to my rescue on

those occasions when I loaded my cart with 100 pounds of seawater and got stuck in the dirt halfway to the surge building). I thank Matt Brown for his good company, laughs, and calm demeanor in the van at sea. I also thank former members of the Bruland lab (Sherry Lippiatt, Matt Brown, Dondra Biller, Tyler Coale, Rob Middag, Vanessa Hatje, Lisa Fischer), former housemates (Joe Murray, Taylor Broek, and Lily Bromberg) and past and present officemates for the company and camaraderie. Finally, I want to thank my family, Mom, Dad, Tom, and Ralph. Their love, support, and company make life good.

The chapters of this dissertation include reprints of the following accepted and in preparation manuscripts:

Chapter 1: Parker, C.E., M.T. Brown, K.W. Bruland, *accepted.* Scandium in the open ocean: a comparison with other group 3 trivalent metals. *Geophysical Research Letters.*

My contribution to this chapter was to perform the sample analysis for Sc, Y, La and Ga, add to the data interpretation, and write the manuscript presented here. Matthew Brown performed the Al analyses and helped edit the manuscript. Kenneth Bruland supervised the sample analysis, directed and supervised the work for this chapter, and provided assistance with the writing the manuscript.

Chapter 2: Parker, C.E., R.U. Shelley, W.M. Landing, K.W. Bruland, *in prep.* Dissolved scandium, yttrium, and lanthanum in the surface waters of the North Atlantic and eastern South Pacific: potential use as an indicator of scavenging intensity. *Journal of Geophysical Research: Oceans.*

I contributed to this chapter by performing all of the dissolved Sc, Y and La analyses, compiling and analyzing data, and writing the manuscript. Rachel Shelley performed aerosol analysis of Sc and La, and William Landing was the principle investigator of the aerosol work. Both Rachel and William provided assistance in data interpretation and manuscript writing. Kenneth Bruland directed and supervised the work for this chapter and provided assistance in writing the manuscript.

Chapter 3: Parker, C.E., T.H. Coale, and K.W. Bruland, *in prep.* Iron limitation off the Oregon Coast.

I contributed to this chapter by performing all of the dissolved Fe analyses shipboard, accessing and imaging the satellite data, and writing the manuscript. Tyler Coale performed the nutrient analyses shipboard. Kenneth Bruland was the chief scientist on the cruise, helped interpret the data, and provided assistance in writing the manuscript.

INTRODUCTION

The past several decades have elucidated some of the important roles that trace metals play in marine biogeochemical cycles. Many trace metals are essential micronutrients, required in small quantities for primary productivity, and a key aspect in marine trace metal research is investigating this nutrient-side: how the trace metal nutrients travel from the crust of the Earth to the surface ocean where they can be utilized by phytoplankton, what makes the trace metals bioavailable, and how the distributions of these trace metals vary by region and over time. Another subset of trace metals are useful as tracers of chemical and physical processes that occur in the ocean; studying these metals can illuminate aspects of water mass movement and mixing, remineralization of biologic material, and scavenging of dissolved seawater constituents onto sinking particles. The two trace metals that are the focus of this dissertation are scandium (Sc), an element that has been studied relatively little in the ocean, and iron (Fe), arguably the most studied trace element in chemical oceanography.

In 1988, director of Moss Landing Marine Laboratories John Martin famously said, "Give me half a tanker of iron, and I will give you an ice age" (Buesseler, 1999). This was the beginning of many large-scale research projects investigating the possibility of fertilizing the ocean with Fe in order to remove CO_2 from the atmosphere. The idea behind John Martin's statement is that there are many regions in the world ocean where there are high concentrations of macronutrients, and yet low levels of primary productivity ("High Nutrient, Lower than expected Chlorophyll" or

HNLC regions). New research at that time (e.g. Martin and Fitzwater, 1988) was revealing that the primary productivity in these HNLC regions was limited by the low concentrations of dissolved Fe, one of the essential micronutrient metals. John Martin's theory was that adding by Fe to the ocean in these HNLC regions, primary productivity would be stimulated and would draw down CO_2 from the atmosphere. The carbon would be incorporated into biological material that would sink to the bottom of the ocean and be sequestered from the atmosphere, thereby ameliorating the rising atmospheric CO_2 levels and decreasing global temperatures. Since then, this theory has been tested many times and from many angles (Martin et al., 1994; Coale et al., 1996; Boyd et al., 2000; Gervais et al., 2002; Tsuda et al., 2003; Coale et al., 2004; Boyd et al., 2004), and while it is clear that primary productivity can be stimulated in HNLC regions with the addition of the correct form of Fe, whether or not the resulting carbon-rich biomass sinks deep enough to be sequestered long-term has proved very difficult to determine. Plus, there are many potential negative side effects of large-scale Fe fertilization, such as toxic algae blooms, changes in community composition up the food chain, low oxygen conditions below the surface due to the additional decaying organic matter, and removal of nutrients besides Fe that would have been utilized elsewhere.

While there are snags with large-scale Fe-fertilization, the research spawned by this investigation has led to a much broader understanding of the oceanic biogeochemical cycle of Fe. One of the surprising aspects of Fe is that it is at trace concentrations (nmol/kg) in the ocean despite being the 4th most prominent element in

crustal material (Wedepohl, 1995). This is in part due to the low solubility of Fe(III), the predominant form of Fe in oxygenated seawater (Wu et al., 2001). There is evidence showing that about 1 billion years ago, the ocean had lower concentrations of dissolved oxygen, which allowed for higher concentrations of Fe to stay dissolved in its more soluble reduced form of Fe(II) (Figure 1) (Anbar, 2008). Some of the evolution of current phytoplankton occurred in this timeframe, which could explain their high Fe requirements, both relative to other metals (Twining and Baines, 2013) and relative to its low ambient concentration.

As biologic material sinks through the ocean it remineralizes: the nutrients that had been incorporated at the surface dissolve. Therefore, biological use transports nutrients downward, and in general deep water has higher concentrations of dissolved nutrients than does the surface water. The macronutrients (nitrate, phosphate, and silicic acid) all have depth profiles with higher concentrations in regions and depths where there has been more time for remineralization to occur (discussed further below) and low concentrations in the surface photic zone. Metals that exhibit these same characteristics are called "nutrient-type" metals (Bruland and Lohan, 2013; Bruland et al., 2014) As a result of this nutrient distribution by depth, regions with upwelling conditions where deeper water moves to the surface are generally nutrient-rich and very productive.

Iron, however, is more complicated. In addition to being utilized at the surface and remineralized as biologic material sinks, Fe also has that low solubility in the modern oxygenated ocean and is particle reactive, meaning that dissolved Fe

associates with sinking particulate matter and is removed from the water column. This process of dissolved constituents associating with particulate matter is called scavenging (Goldberg, 1954). Iron is designated a "hybrid-type" metal, with biological utilization and particle reactivity both playing important roles in its oceanic distribution (Bruland and Lohan, 2003; Bruland et al., 2014). Much of the dissolved Fe input to the ocean from remineralization is removed from the water column by scavenging and the concentration of Fe remains low. Therefore many HNLC regions are where deep water is upwelled to the surface photic zone resulting in elevated macronutrient concentrations in the surface and insufficient Fe for the phytoplankton to make full use of the available macronutrients.

Eastern boundary regions, such as the California Current System on the eastern boundary of the North Pacific subtropical gyre, are examples of upwelling regions. In eastern boundary regions, equatorward alongshore winds result in Ekman transport of the surface water offshore, and this deficit of water near shore leads to coastal upwelling of deep-water to the surface. In the California Current System there is a strong seasonal aspect to the coastal upwelling conditions with the equatorward winds occurring during the spring and summer months (Huyer, 1983; Lynn and Simpson, 1987; Strub et al., 1987). Upwelling occurs both through this coastal upwelling, and through slower wind-stress curl induced upwelling, where the winds increase in strength moving offshore and the divergence in Ekman transport is compensated by vertical transport upward (Figure 2) (Rykazewski and Checkley,

2008). Wind stress curl induced upwelling is slower but more pervasive than coastal upwelling.

One of the major factors in whether upwelling in eastern boundary regions results in Fe-limiting conditions is the width of the continental shelf at the location of upwelling (Chase et al, 2007; Biller et al., 2013; Hutchins et al., 1998). In the winter, heavy rains and storms increase river flow into the ocean, and with it comes high concentrations of sediment and Fe input. A large percentage of that Fe sinks to 50-90 m mud belts (Wheatcroft et al., 1997; Xu et al., 2002), but can be re-suspended and brought to the surface by coastal upwelling conditions in the spring and summer months (Johnson et al., 1999). In regions with wider continental shelf mud belts, there is more surface area on which the riverine Fe can be caught and more contact between the continental shelf and the upwelling water through which Fe can be upwelled (Figure 3). Primary productivity has been linked with wider continental shelf width and higher river input (Figure 4) (Chase, 2007), and Bruland et al. (2005) and Kudela et al. (2006) have noted a steep drop in surface dissolved iron concentration past the shelf break. There is significant evidence (Biller et al., 2013; Bruland et al. 2001; Firme et al., 2003; Hutchins et al., 1998; King and Barbeau, 2007) of Fe-limitation in some regions of the central and southern California Current System. The northern California Current System off of northern Oregon and Washington has been shown to be rich in Fe, due to the relatively wide continental shelf and large amount of sediment input from the Columbia River (Bruland et al., 2008).

Chapter 3, titled “Iron limitation off the coast of Oregon,” provides evidence for Fe-limitation of coastal diatoms to exist further north in the California Current System than previously identified, off of coast of southern Oregon near Cape Blanco. The sampling location was offshore of the continental shelf break, in a region with moderate shelf width and river input. Estimations of low Fe concentrations limiting the growth rate and biomass accumulation of coastal diatoms were calculated as in Biller et al. (2013). The results provide evidence for both types of Fe-limitation of coastal diatoms, and suggest that even oceanic diatoms, with a lower requirement for Fe than coastal diatoms, would be limited in biomass accumulation by Fe in this region. This chapter shows evidence of Fe-limitation further north in the California Current System than previously known, which could be a significant contributor to global models of primary productivity.

The work from Chapter 3 was part of a collaborative research cruise along the California and Oregon coastlines in July 2014. The cruise focused on the use of Fe by phytoplankton, approached from many angles with microbial biologists, phytoplankton ecologists, zooplankton biologists, isotope chemists, dissolved trace metal, particulate trace metal, and ligand trace metal chemists all working together to piece together a better understanding of the system. Due to this high level of collaboration, the dissolved Fe data collected and analyzed on the cruise that contributed to this dissertation chapter also supported five oral presentations at the February 2016 Ocean Sciences meeting in New Orleans.

In contrast to this vast array of research into oceanic Fe cycling, prior to the work of this dissertation the only modern published data for dissolved Sc was one depth profile in the North Central Pacific Ocean (Amakawa et al., 2007). There were also several dissolved Sc profiles published in the 1970s (Spencer et al., 1970; Brewer et al., 1972), but the trace metal clean methods of the time were not able to provide detection limits lower than the samples. One of the main goals of this dissertation was to expand upon the limited knowledge of dissolved Sc in the ocean with a basic understanding of its global distribution and reactivity (Chapter 1), and to investigate possible uses of dissolved Sc as an indicator of chemical processes occurring in the ocean (Chapters 1 and 2).

Metals are categorized into different "types" based on patterns of their distribution compared with the age of the deep water (Bruland and Lohan, 2003; Bruland et al., 2014). Deep water is said to be "older" when more time has passed since it was last at the surface. The more time the water has spent away from the surface, the more time there has been for the dissolved concentration of metals to be impacted by input from remineralization and removal from scavenging onto particles. As mentioned previously, the distribution of nutrient-type metals is mostly affected by their role as a nutrient, and due to remineralization of organic matter they increase in concentration with age of the deep water (Figure 5). Scavenged-type metals have distributions that are mostly governed by their high particle reactivity and removal from the water column with time, so they do the opposite (Figure 6). Hybrid-type

metals such as Fe have distributions that are significantly influenced by both processes (Figure 7).

Chapter 1 of this dissertation (Parker, C.E., Brown, M.T., Bruland, K.W. 2016; Scandium in the open ocean: A comparison with other group 3 trivalent metals, *accepted for publication*) focuses on the distribution and reactivity of Sc in the open ocean. This work presents dissolved Sc profiles from the North Atlantic, the South Pacific, and the North Pacific, and identifies Sc as a hybrid-type metal like Fe, with input of dissolved Sc from remineralization about balanced out by removal through scavenging onto particles. This is the first study to publish reliable dissolved Sc data from multiple regions of the world, providing a basic understanding of the distribution and reactivity of dissolved Sc.

For a given analyte, higher input relative to removal leads to longer oceanic residence times. The difference in deep-water concentration between the North Atlantic (relatively young deep water) and the North Pacific (relatively old deep water) gives an indication of the balance between input from remineralization and removal from scavenging. Scavenged-type metals, with high particle reactivity and a correspondingly high scavenging removal term, have short oceanic residence times relative to the age of the deep water. Nutrient-type metals have long residence times relative to the age of the deep water (although the residence times of major ions in the ocean such as Mg^{2+} and Ca^{2+} are longer still). By comparing the difference between deep-water concentrations of dissolved Sc in the North Atlantic and the North Pacific with those of other metals (yttrium (Y), lanthanum (La), gallium (Ga), and aluminum

(Al)), and using previous estimations for the residence times of those metals (Orians and Bruland, 1985; Orians and Bruland, 1988; Bruland et al., 1994; Johnson et al., 1997; Alibo and Nozaki, 1999) we are able to infer an estimate of the oceanic residence time of dissolved Sc in Chapter 1.

One of the intriguing aspects of Sc in the ocean is its similarity to Fe. Byrne (2002) calculates that both speciate predominantly in the form Metal-$(OH)_3^0$. This implies that their reactivity in the ocean might be similar, and indeed Chapter 1 shows that they do have similar deep-water Atlantic to Pacific ratios. Since there are no known biological uses of Sc, and Sc and Fe have a similar distribution and reactivity in the ocean, Chapter 1 also suggests that the Sc distribution could represent the "non-nutrient" side of the elusive oceanic Fe cycle and that it could be used to help tease apart aspects of the complicated and important biogeochemistry of Fe.

Chapter 2 of this dissertation is titled, "Dissolved scandium, yttrium, and lanthanum in the surface waters of the North Atlantic and eastern South Pacific: potential use as an indicator of scavenging intensity," and will soon be submitted for publication to Journal of Geophysical Research: Oceans. Samples for this chapter were taken on a transect across the North Atlantic subtropical gyre as part of the GEOTRACES program. This chapter focuses on whether the difference in particle reactivity between Sc and its periodic table group-mates Y and La can be used to provide an indication of scavenging intensity in the surface ocean. Other scavenging indicators such as Al, Ga, $^{231}Pa/^{230}Th$, ^{234}Th, ^{228}Th, and $^{210}Po/^{210}Pb$ have been widely used to investigate scavenging in the water column (e.g. Bacon and Anderson, 1982;

Henderson and Slowey, 2000; Savoye et al., 2006; Rutgers v.d. Loeff and Geibert, 2008). Each scavenging indicator provides information on specific timescales and often about specific particle composition, so new indicators can provide unique insights.

Yttrium and La are well-characterized nutrient-type metals (de Baar et al., 1985; Alibo et al., 1999), while Sc is a hybrid-type that is much more particle reactive (Parker et al., accepted). If Y/Sc and La/Sc are input to the surface ocean in constant ratios, than any variation in the dissolved Y/Sc and La/Sc that we observe is likely due to Sc removal by scavenging. Atmospheric input of dust is one of the major pathways for trace metals to get from the land into the ocean, and mineral dust carried on the westerly winds from the Sahara provides the surface North Atlantic Ocean with one of the largest degrees of atmospheric dust input globally (figure 8) (e.g. Prospero and Carlson, 1972; Jickells et al., 2005). Aerosol input of mineral dust is presumably the dominant source for many metals into the surface North Atlantic. Ratios of Sc, Y and the lanthanides have often been used to identify the provenance of dust (e.g. Pease and Tchakerian, 2002), so Saharan dust likely has relatively consistent ratios of Sc, Y and La. From this it follows that Sc, Y and La are likely input to the surface North Atlantic in roughly constant ratios (which will be investigated in Chapter 2), and that the deviation from those ratios is likely due to Sc removal by scavenging. Chapter 2 investigates the possibility of using Sc removal and the resulting offset in Y/Sc and La/Sc ratios as an indicator of scavenging intensity.

Overall, this dissertation provides new investigation into dissolved Sc and Fe in the ocean. Chapters 1 and 2 contribute significantly to the total knowledge of the oceanic distribution and reactivity of dissolved Sc and investigate two potential applications for this new knowledge: a promising scavenging indicator and the potential to help tease apart aspects of the oceanic Fe cycle. Chapter 3 expands on previous work on Fe-limitation in the California Current System with evidence for Fe-limitation of coastal diatoms off of Cape Blanco in southern Oregon, indicating that the Fe-limitation mosaic of the southern California Current System extends further north than previously known.

References

Alibo, D. S., and Y. Nozaki (1999), Rare earth elements in seawater: Particle association, shale-normalization, and Ce oxidation, Geochim. Cosmochim. Ac., 63 [3/4], 363-372, doi:10.1016/S0016-7037(98)00279-8.

Amakawa, H., M. Nomura, K. Sasaki, Y. Oura, and M. Ebihara (2007), Vertical distribution of scandium in the north central Pacific, Geophys. Res. Lett., 34, LL11606, doi:10.1029/2007GL029903.

Anbar, A.D. (2008), Elements and evolution, Science, 322, 1481-1483, doi: 10.1126/science.1163100.

Bacon, M.P., and R.F. Anderson (1982), Distribution of thorium isotopes between dissolved and particulate forms in the deep sea, J. Geophys. Res., 87, 2045-2056, doi:10.1029/JC087iC03p02045.

Brewer, P. G., D.W. Spencer, and D.E. Robertson (1972), Trace element profiles from the GEOSECS-II test station in the Sargasso Sea, Earth Planet. Sci. Lett., 16: 111-116, doi:10.1016/0012-821X(72)90243-9.

Biller, D.V., T.H. Coale, R.C. Till, G.J. Smith, and K.W. Bruland (2013), Coastal iron and nitrate distributions during the spring and summer upwelling season in the central California Current upwelling regime, Cont. Shelf Res., 66, 58-72, doi: 10.1016/j.csr.2013.07.003.

Boyd, P. W., A.J. Watson, C.S. Law, E.R. Abraham, T. Trull, R. Murdoch, D.C.E. Bakker, A.R. Bowie, K.O. Buesseler, H. Chang, M. Charrette, P. Croot, K. Downing, R. Frew, M. Gall, M. Hadfield, J Hall, M. Harvey, G. Jameson, J. LaRoche, M. Liddicoat, R. Ling, M.T. Maldonado, R.M. McKay, S. Nodder, S. Pickmere, R. Pridmore, S. Rintoul, K. Safi, P. Sutton, R. Strzepek, K. Tanneberger, S. Turner, A. Waite, and J. Zeldis (2000), A mesoscale phytoplankton bloom in the polar Southern Ocean stimulated by iron fertilization, Nature, 407, 695–702, doi: 10.1038/35037500.

Boyd, P. W., (2004), Ironing out algal issues in the Southern Ocean, Science, 304, 396-397, doi:10.1126/science.1092677.

Bruland, K.W., K.J. Orians, and J.P. Cowen (1994), Reactive trace metals in the stratified central North Pacific, Geochim. Cosmochim. Ac., 58(15), 3171-3182, doi:10.1016/0016-7037(94)90044-2.

Bruland, K.W., E.L. Rue, and G.J. Smith (2001), Iron and macronutrients in California coastal upwelling regimes: implications for diatom blooms, Limnol. Oceanogr., 46, 1661–1674, doi:10.4319/lo.2001.46.7.1661.

Bruland, K. W., and Lohan, M. C. (2003), Controls of trace metals in seawater, Treatise on Geochemistry. Elsevier Ltd., V6, [ISBN: 0-08-044341-9], 23-47.

Bruland, K.W., R. Middag, and M.C. Lohan (2014), Controls of trace metals in seawater, Treatise on Geochemistry (2nd edition), Elsevier, Oxford, [ISBN: ISBN: 978-0-08-098300-4],19-51, doi:10.1016/B978-0-08-095975-7.00602-1.

Buesseler, K.O. (1999), Fertilizing the ocean with iron, Woods Hole Oceanographic Institute Annual Report, 22-23.

Chase, Z., P.G. Strutton, and B. Hales (2007), Iron links river runoff and shelf width to phytoplankton biomass along the US West Coast, Geophys. Res. Lett., 34, LO4607, doi:10.1029/2006GL028069.

Coale, K. H., K.S. Johnson, S.E. Fitzwater, R.M. Gordon, S. Tanner, F.P. Chavez, L. Ferioli, C. Sakamoto, P. Rogers, F. Millero, P. Steinburg, P. Nightingale, D. Cooper, W.P. Cochlan, M.R. Landry, J. Constantinou, G. Rollwagen, A. Trasvina, and R. Kudela (1996), A massive phytoplankton bloom induced by an ecosystem-scale iron fertilization experiment in the equatorial Pacific Ocean, Nature, 383, 495–501, doi:10.1038/383495a0.

Coale, K. H., K.S. Johnson, F.P. Chavez, K.O Buesseler, R.T. Barber, M.A. Brzezinski, W.P. Cochlan, F.J. Millero, P.G. Falkowski, J.E. Bauer, R.H. Wanninkhof, R.M. Kudela, M.A. Altabet, B.E. Hales, T. Takahashi, M.R. Landry, R.R. Bidigare, X. Wang, Z. Chase, P.G. Strutton, G.E. Friederich, M.Y. Gorbunov, V.P. Lance, A.K. Hilting, M.R. Hiscock, M. Demarest, W.T. Hiscock, K.F. Sullivan, S.J. Tanner, R.M. Gordon, C.N. Hunter, V.A. Elrod, S.E. Fitzwater, J.L. Jones, S. Tozzi, M. Koblizek, A.E. Roberts, J. Herndon, J. Brewster, N. Lanizinsky, G. Smith, D. Cooper, D. Timothy, S.L. Brown, K.E. Selph, C.C. Sheridan, B.S. Twining, Z.I. Johnson (2004), Southern Ocean Iron Enrichment Experiment: Carbon cycling in high- and low-Si waters, Science, 304, 408–414, doi: 10.1126/science.1089778.

de Baar, H.J.W., M.P. Bacon, P.G. Brewer, and K.W. Bruland (1985), Rare earth elements in the Pacific and Atlantic Oceans, Geochim. Cosmochim. Ac., 49, 1943-1959, doi:10.1016/0016-7037(85)90089-4.

Firme, G.F., E.L. Rue, D.A. Weeks, K.W. Bruland, and D.A. Hutchins (2003), Spatial and temporal variability in phytoplankton iron limitation along the California

coast and consequences for Si, N, and C biogeochemistry, Global Biogeochem. Cycles, 17, 1016, doi:10.1029/2001GB001824.

Gervais, F., U. Riebesell, and M. Y. Gorbunov (2002), Changes in primary productivity and chlorophyll a in response to iron fertilization in the Southern Polar Frontal Zone, Limnol. Oceanogr., 47, 1324–1335, doi:10.4319/lo.2002.47.5.1324.

Goldberg, E.D. (1954), Marine Geochemistry 1: Chemical scavengers of the sea, J. Geol., 62(3), 249-265.

Henderson, G.M., and N.C. Slowey (2000), Evidence from U-Th dating against Northern Hemisphere forcing of the penultimate deglaciation, Nature, 404, 61-66, doi: 10.1038/35003541.

Huyer, A. (1983), Coastal upwelling in the California Current System, Prog. Oceanogr., 12, 259–284, doi:10.1016/0079-6611(83)90010-1.

Hutchins, D.A., G.R. Ditullio, Y. Zhang, and K.W. Bruland (1998), An iron limitation mosaic in the California upwelling regime, Limnol. Oceanogr., 43, 1037–1054, doi: 10.4319/lo.1998.43.6.1037.

Jickells, T.D., Z.S. An, K.K. Anderson, A.R. Baker, G. Bergametti, N. Brooks, J.J. Cao, P.W. Boyd, K.A. Hunter, H. Kawahata, N. Kubliay, J. laRoche, P.S. Liss, N. Mahowald, J.M. Prospero, A.J. Ridgwell, I. Tegen, R. Torres (2005), Global iron connections between desert dust, ocean biogeochemistry, and climate, Science, 308, 67-71, doi:10.1126/science.1105959.

Johnson, K.S., R.M. Gordon, and K.H. Coale (1997), What controls dissolved iron concentrations in the world ocean?, Mar. Chem., 57, 137-161, doi:10.1016/S0304-4203(97)00043-1.

Johnson, K.S., F.P. Chavez, and G.E. Friederich (1999), Continental-shelf sediment as a primary source of iron for coastal phytoplankton, Nature, 398, 697–700, doi:10.1038/19511.

King, A.L., and K. Barbeau (2007), Evidence for phytoplankton iron limitation in the southern California Current System, Mar. Ecol.-Prog. Ser., 342, 91–103, doi:10.3354/meps342091.

Kudela, R., N. Garfield, and K. Bruland (2006), Bio-optical signatures and biogeochemistry from intense upwelling and relaxation in coastal California. Deep-Sea Research Part II 53:2,999–3,022, doi:10.1016/j.dsr2.2006.07.010.

Lynn, R.J., and J. J. Simpson (1987), The California Current System: the seasonal variability of its physical characteristics, J. Geophys. Res., 92(C12), 12947–12966, doi:10.1029/JC092iC12p12947.

Martin, J., and S. Fitzwater (1988), Iron deficiency limits phytoplankton growth in the northeast Pacific subarctic, Nature, 331, 341–343, doi:10.1038/331341a0.

Martin, J. H., K.H. Coale, K.S. Johnson, S.E. Fitzwater, R.M. Gordon, S.J. Tanner, C.N. Hunter, V.A. Elrod, J.L. Nowicki, T.L. Coley, R.T. Barber, S. Lindley, A.J. Watson, K. van Scoy, C.S. Law, M.I. Liddicoat, R. Ling, T. Stanton, J. Stockel, C. Collins, A. Anderson, R. Bidigare, M. Ondrusek, M. Latasa, F.J. Millero, K. Lee, W. Yao, J.Z. Zhang, G. Friederich, C. Sakamoto, F Chavez, K. Buck, Z. Kolber, R. Greene, P. Falkowski, S.W. Chisholm, F. Hoge, R. Swift, J. Yungel, S. Turner, P. Nightingale, A. Hatton, P. Liss, and N.W. Tindale (1994), Testing the iron hypothesis in ecosystems in the equatorial Pacific, Nature, 371,123–129, doi:10.1038/371123a0.

Orians, K. J. and K. W. Bruland (1985), Dissolved aluminum in the central North Pacific, Nature, 316 (1), 427-429, doi:10.1038/316427a0.

Orians, K. J., and K. W. Bruland (1988), Dissolved gallium in the open ocean, Nature, 332(21), 717-719, doi:10.1038/332717a0.

Parker, C.E., M.T. Brown, and K.W. Bruland (accepted), Scandium in the open ocean: A comparison with other group 3 trivalent metals, Geophys. Res. Lett., doi:10.1002/2016GL067827.

Pease, P.P., and V.P. Tchakerian (2002), Composition and sources of sand in the Wahiba Sand Sea, Sultanate of Oman, Ann. Assoc. Am. Geogr., 92, 416–434, doi:10.1111/1467-8306.00297.

Prospero, J.M., and T.N. Carlson (1972), Vertical and areal distribution of Saharan dust over the Western Equatorial North Atlantic Ocean, J. Geophys. Res., 77[27], 5255-5265, doi:10.1029/JC077i027p05255.

Rutgers van der Loeff, M.M., and W. Geibert (2008), U- and Th-series nuclides as tracers of particle dynamics, scavenging and biogeochemical cycles in the oceans, in U-Th Series Nuclides in Aquatic Systems, 227–268, Elsevier, doi:10.1016/S1569-4860(07)00007-1.

Rykazewski, R.R., and D.M. Checkley (2008), Influence of ocean winds on the pelagic ecosystem in upwelling regions, Proceedings of the National Academy of Sciences, 105(6), 1965-1970, doi:10.1073/pnas.0711777105.

Savoye, N., C. Benitez-Nelson, A.B. Burd, J.K. Cochran, M. Charette, K.O. Buesseler, G.A. Jackson, M. Roy-Barman, S. Schmidt, and M. Elskens (2006), 234Th sorption and export models in the water column: a review, Mar. Chem., 100, 234-249, doi:10.1016/j.marchem.2005.10.014.

Spencer, D.W., D.E. Robertson, K.K. Turekian, and T.R. Folsom (1970), Trace element calibrations and profiles at the Geosecs test station in the Northeast Pacific Ocean, J. Geophys. Res., 75: 7688, doi:10.1029/JC075i036p07688.

Strub, P.T., J.S. Allen, A. Huyer, and R.L. Smith (1987), Large-scale structure of the spring transition in the coastal ocean off western North America, J. Geophys. Res., 92(C2), 1527–1544, doi:10.1029/JC092iC02p01527.

Tsuda, A., S. Takeda, H. Saito, J. Nishioka, Y. Nojiri, I. Kudo, H. Kiyosawa, A. Shiomoto, K. Imai, T. Ono, A. Shimamoto, D. Tsumune, T. Yoshimura, T. Aono, A. Hinuma, M. Kinugasa, K. Suzuki, Y. Sohrin, Y. Noiri, H. Tani, Y. Deguchi, N. Tsurushima, H. Ogawa, K. Fukami, K. Kuma, and T. Saino (2003), A mesoscale iron enrichment in the western subarctic Pacific induces a large centric diatom bloom, Science, 300, 958–961, doi:10.1126/science.1082000.

Twining, B.S., and S.B. Baines (2013), The trace metal composition of marine phytoplankton, Annu. Rev. Marine. Sci., 5, 191-215, doi:s10.1146/annurev-marine-121211-172322.

Wedepohl, K. H., (1995), The composition of the continental crust. Geochim. Cosmochim. Acta 59, 1217–1232, doi: 10.1016/0016-7037(95)00038-2.

Wheatcroft, R.A., C.K. Sommerfield, D.E. Drake, J.C. Borgeld, and C.A. Nittrouer (1997), Rapid and widespread dispersal of flood sediment on the northern California margin, Geology, 25(2), 163–166, doi:10.1130/0091-7613(1997)025<0163:RAWDOF>2.3.CO;2.

Wu, J., E. Boyle, W. Sunda, and L.-S. Wen (2001), Soluble and colloidal iron in the oligotrophic North Atlantic and North Pacific, Science, 293(5531), 847-849, doi:10.1126/science.1059251.

Xu, J.P., M. Noble, and S.L. Eittreim (2002), Suspended sediment transport on the continental shelf near Davenport, California, Mar. Geol., 181, 171–193, doi:10.1016/S0025-3227(01)00266-3.

Figures

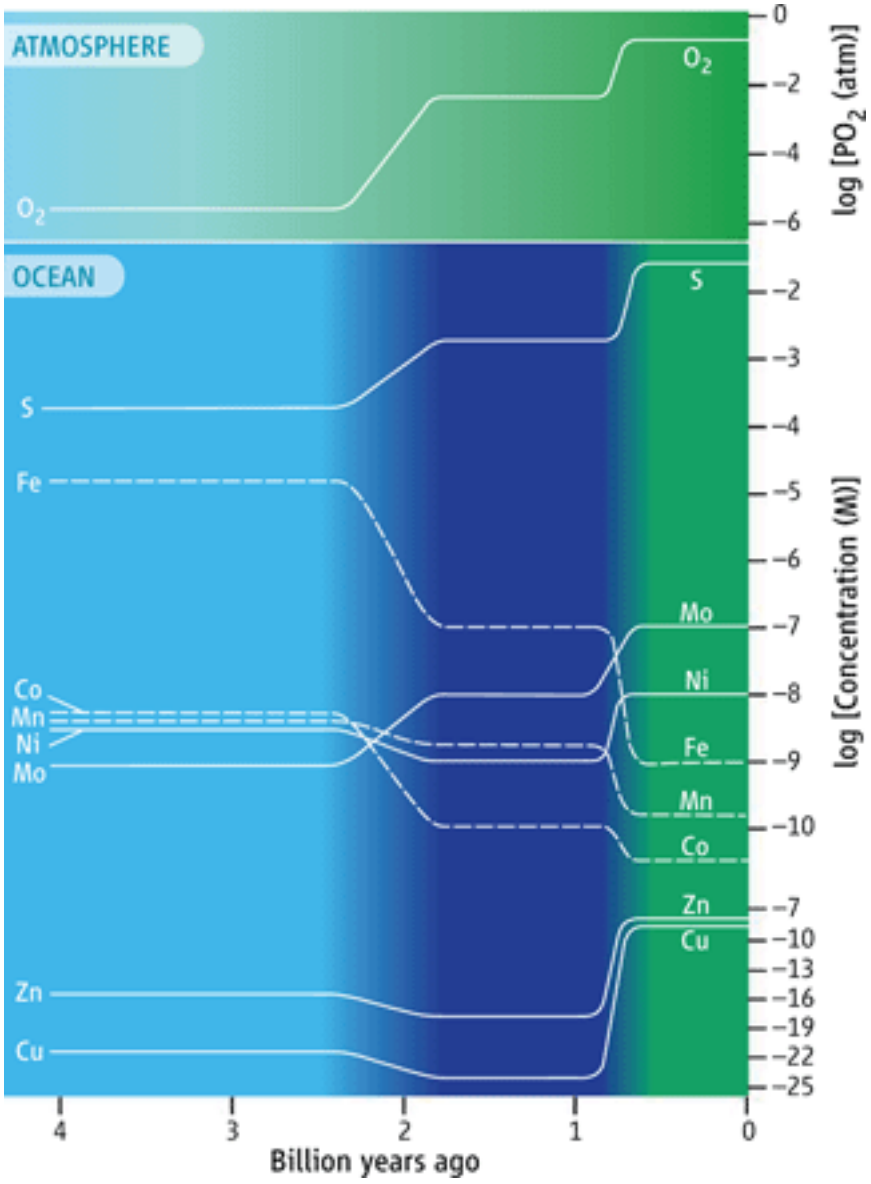

Figure 1: Reproduced with permission from Anbar, 2008, this figure shows the major changes in element concentrations from the ancient ocean to present. Color gradations indicate the transition from anoxic (light blue) to moderate oxygen (dark blue), to complete ocean oxygenation (green). Note the significant decrease in the Fe concentration as the ocean becomes oxygenated.

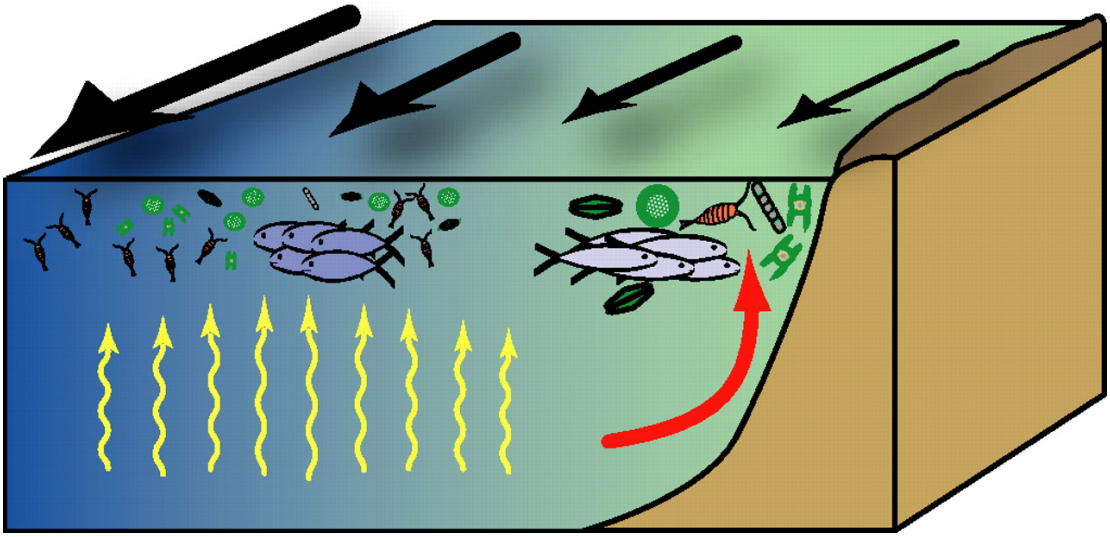

Figure 2: From Rykaczewski and Checkley, 2008, this schematic shows coastal upwelling (red arrow) and wind stress curl induced upwelling (yellow arrows). As the winds move equatorward, Ekman transport moves the surface water offshore. This is balanced out by vertical transport of deep water upward. The wind stress curl of stronger winds offshore leads to a divergence of Ekman transport that is also balanced out with upwelling. Wind stress curl upwelling is slower but more pervasive than coastal upwelling. Figure Copyright (2008) National Academy of Sciences, U.S.A.

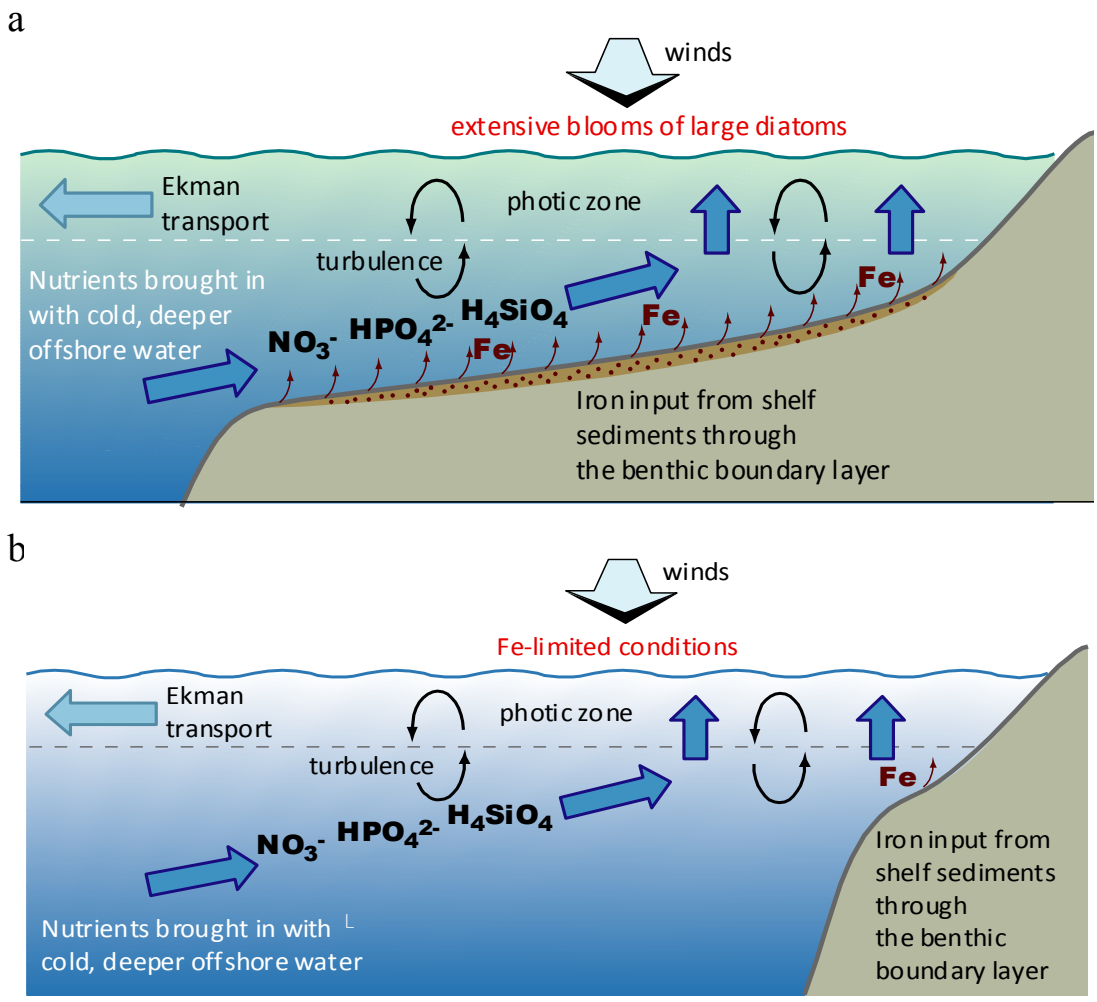

Figure 3: Schematic depicting coastal upwelling over wide (a) and narrow (b) shelf widths. In regions with narrow shelf widths (b), there is less Fe upwelled relative to the macronutrients, and Fe-limitation often occurs.

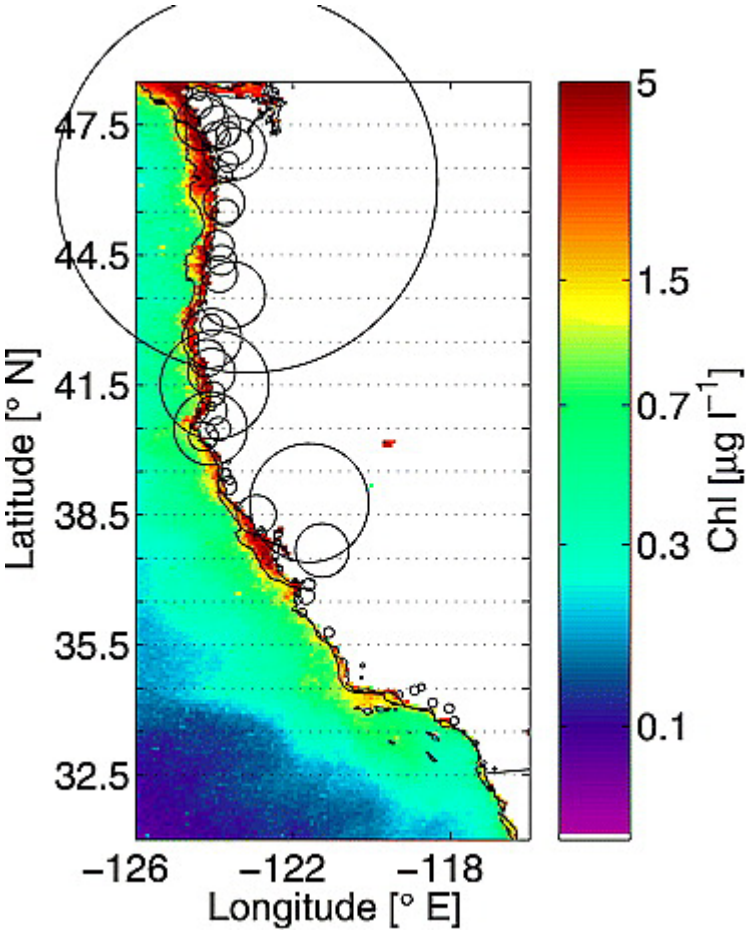

Figure 4: Reproduced with permission from Chase et al., 2007, this figures shows river input volume (larger circles correspond with greater volume and the center of the circle is the measured location) overlaid on surface chlorophyll concentration along the California Current System. Regions with higher (red) chlorophyll near shore generally have higher river input.

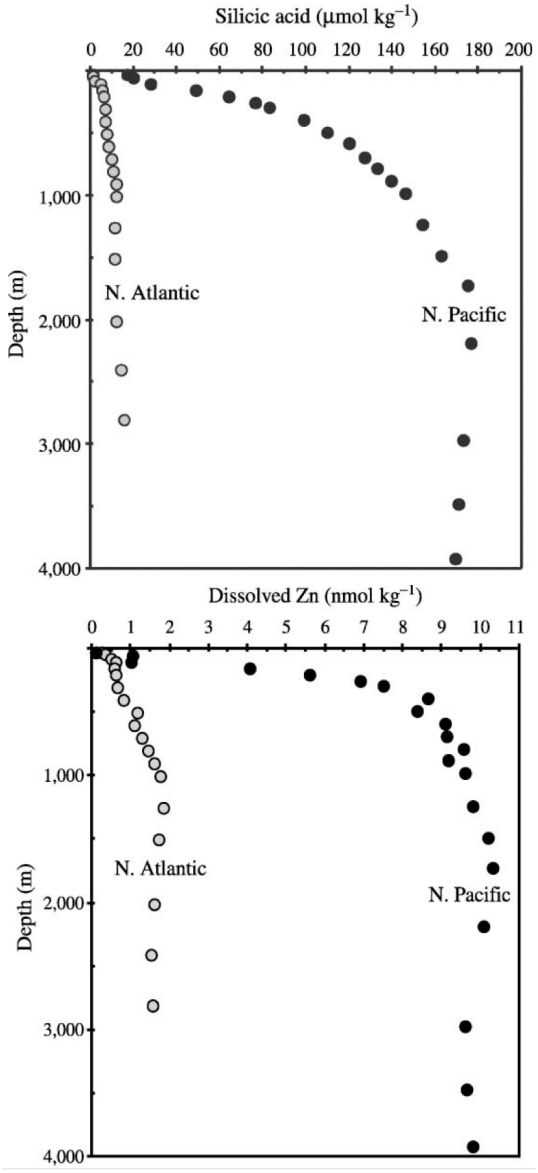

Figure 5: From Bruland and Lohan, 2003, this figure shows depth profiles of silicic acid and dissolved Zn in the North Atlantic (white circles, data from Martin et al., 1993) and North Pacific (black circles, data from Martin et al., 1989). Silicic acid is a macronutrient and Zn a nutrient-type metal. Both show low concentrations in the surface and higher deep-water concentrations in the older North Pacific deep water than in the younger North Atlantic deep water.

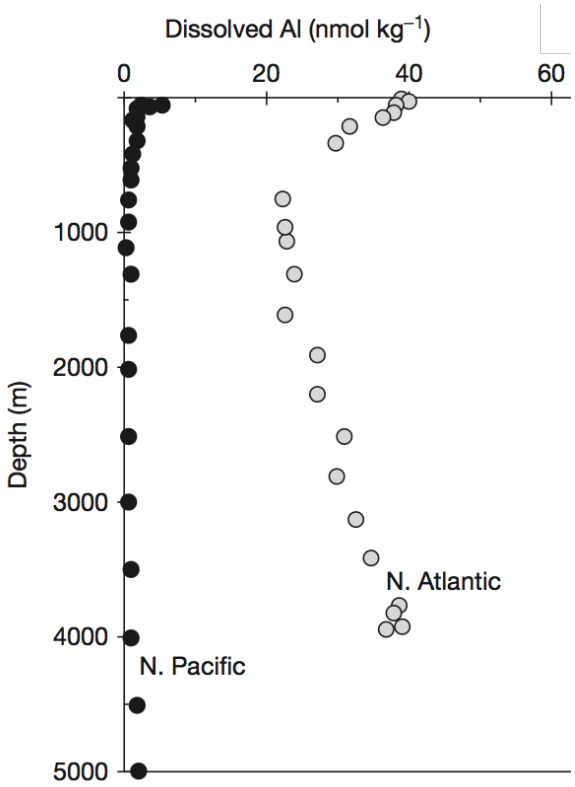

Figure 6: From Bruland et al., 2014, this figure shows depth profiles of dissolved Al in the North Atlantic (white circles, data from Hydes, 1979) and North Pacific (black circles, data from Orians and Bruland, 1986). Aluminum depicts typical scavenged-type profiles, higher in concentration in the surface and decreasing in deep-water concentration from the North Atlantic to the North Pacific.

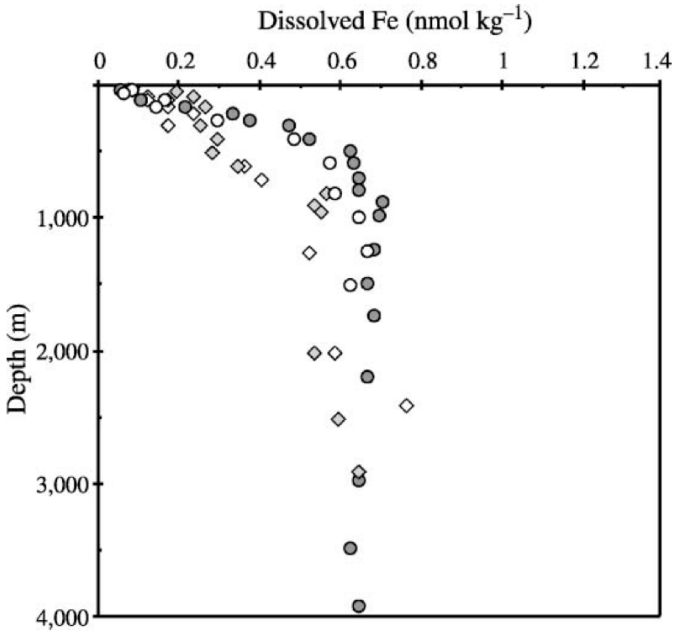

Figure 7: From Bruland and Lohan, 2003, this figure shows depth profiles of dissolved Fe in the North Atlantic (diamonds, data from Martin et al., 1993) and in the North Pacific (circles, data from Martin et al., 1989). Iron is a hybrid-type metal: while resembling a nutrient profile with lower concentrations in the surface, the deep-water concentration of Fe does not increase dramatically from the North Atlantic to the North Pacific as the macronutrients and nutrient-type metals do.

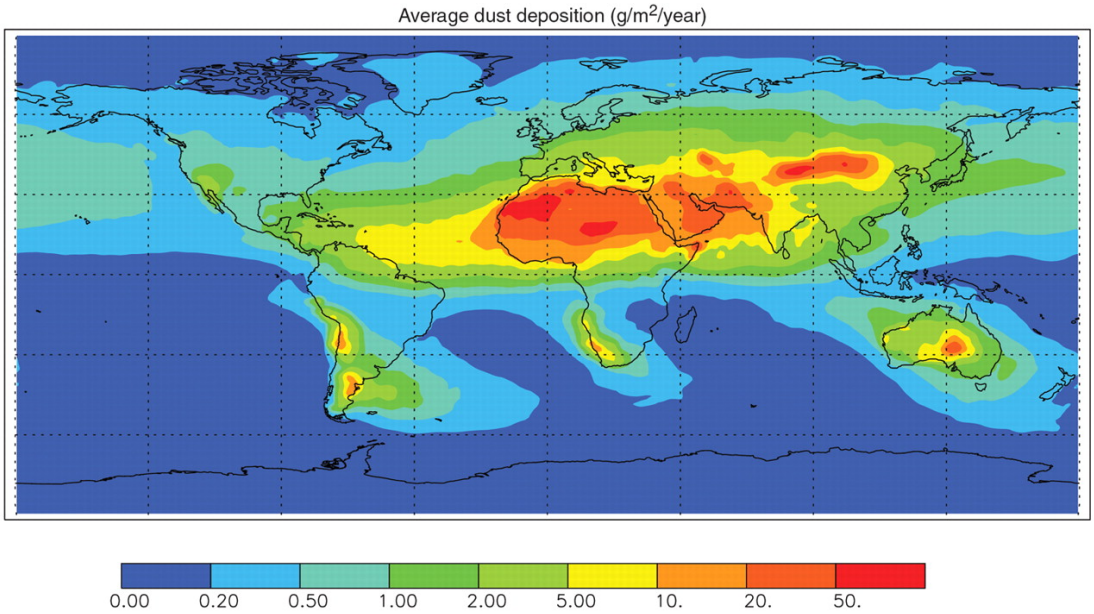

Figure 8: Reproduced with permission from Jickells et al., 2005, this figure shows modeled dust fluxes to the world ocean. Note the major source of dust from the Sahara to the North Atlantic.

CHAPTER 1: SCANDIUM IN THE OPEN OCEAN: A COMPARISON WITH OTHER GROUP 3 TRIVALENT METALS

Claire E. Parker, Matthew T. Brown and Kenneth W. Bruland

Accepted for publication in *Geophysical Research Letters*

Abstract

Little is known about the distribution of scandium (Sc) in the open ocean. Since the 1970s there has been only one published depth profile of dissolved Sc. The work presented here reports depth profiles of dissolved Sc from GEOTRACES cruises in the North Atlantic, North Pacific and South Pacific. This work also compares the reactivity of Sc with its trivalent periodic table group-mates in Group IIIB, yttrium (Y) and lanthanum (La), and Group IIIA, aluminum (Al) and gallium (Ga). Yttrium and La are classic nutrient-type metals that increase in concentration in aging deep water; Al and Ga are classic scavenged-type metals that do the opposite. Results indicate that Sc is a hybrid-type metal with an inferred residence time on the order of 1000 years, and that Sc's inorganic speciation and reactivity are similar to Fe's and have the potential to give insights into the non-nutrient side of oceanic Fe cycling.

1. Introduction

The marine geochemistry of dissolved scandium (Sc) is poorly understood. The only modern study to publish a depth profile of Sc (Amakawa et al., 2007) showed that in the North Central Pacific, Sc exhibits characteristics of a nutrient-type element with lower concentrations in the surface that increase with depth. The same study calculated that Sc's depth profile is highly correlated with those of yttrium (Y) and lanthanum (La) (correlation coefficients greater than 0.93), which are known to have nutrient-like vertical profiles with deep-water concentrations increasing from the Atlantic to the Pacific (Alibo et al., 1999; de Baar et al., 1985). However, Amakawa et al. (2007) also found that dissolved Y/Sc and La/Sc ratios in the North Central Pacific indicated depleted Sc compared to loess crustal values (reported by Taylor et al. (1983)), suggesting a sink of dissolved Sc in excess of the dissolved Y and La sinks. Amakawa et al. (2007) noted that this depletion of Sc relative to Y and La combined with Sc's positive correlations with Y and La nutrient-type depth profiles support conflicting views on the reactivity of Sc compared to Y and La. This study addresses the question of Sc's particle reactivity and investigates the potential use of Sc distributions.

Scandium, Y, and La are three of the four elements usually agreed to constitute Group IIIB of the periodic table (there is some discussion on where the f block fits in) (Jensen, 1982; Lavelle, 2008). (We choose to use the old IUPAC notation for periodic table groups in order to highlight the similarity between Group IIIB and Group IIIA (called Group 3 and Group 13, respectively, in the new IUPAC

notation) (Fluck, 1988). In this work, we use the term "Group 3" to refer to both Group IIIA and Group IIIB elements.) Group IIIB metals are characterized by their stable oxidation in the +3 state, but there are several lines of evidence suggesting that Sc's reactivity in the ocean may be distinct from the other two. Using ionic strength corrected thermodynamic constants for many possible aquatic chemical reactions, Byrne (2002) calculated that while all three are highly complexed in seawater at a +3 oxidation state, Sc is dominantly hydrolyzed as the neutral $Sc(OH)_3^0$ species, whereas Y and La are dominantly complexed with carbonate as Metal-CO_3^+. This difference in complexation implies a corresponding difference in reactivity in the ocean. There is also evidence of differences in reactivity between Sc and the other two from the work of Chen et al. (1996), which concluded that artificial marine particles more actively adsorbed Sc than Y or some lanthanides.

Scandium's hydrolyzed inorganic speciation in seawater makes it similar to aluminum (Al), iron (Fe), gallium (Ga), titanium (Ti), and thorium (Th), all elements prone to particle scavenging. Scandium's similarity to these reactive metals in seawater, particularly the other trivalent Group 3 metals Al and Ga, is another indication of Sc's potential particle reactivity. Byrne (2002) calculates that Ga is predominantly $Ga(OH)_4^-$, and Al is either $Al(OH)_3^0$ or $Al(OH)_4^-$, depending on the pH ($pK_4^* = 7.7$). Balistrieri et al. (1981) found a relationship between the stability constants of metal hydroxide complexes and the stability constants of metal interactions with oxides or organic compounds. Furthermore, the Sc^{3+} ionic radius is larger than those of Ga^{3+} and Al^{3+}, resulting in a lower charge density (Shannon,

1976). Both the calculated degrees of hydroxide complexation and the relative ionic sizes of these metals suggest that Sc may be less particle reactive than Al and Ga.

Byrne (2002)'s work indicates that both Sc and inorganic Fe are predominantly in the neutral Metal-$(OH)_3^0$ form (although Byrne notes that there are some problems in the analytical procedure used to determine the inorganic speciation of Fe), suggesting they may have similar reactivity in the ocean. The biogeochemical cycling of Fe and its importance as the limiting micronutrient in much of the World Ocean have been widely investigated since the late 1980s (e.g. Martin et al., 1989; Coale et al., 1996; Moore et al., 2002). Despite this interest and its importance, the oceanic Fe cycle has proved difficult to fully constrain. In addition to particle scavenging, Fe cycling is complicated by organic complexation with strong Fe(III)-binding organic ligands and biological utilization (Rue and Bruland 1995, 1997; Gledhill and van den Berg, 1994; van den Berg, 1995; Wu and Luther, 1995; Gledhill and Buck, 2012). Scandium may also form organic complexes in the ocean, potentially with the same Fe-binding ligands; Rogers et al. (1980) found evidence of Sc competing with Fe for binding sites on the siderophore enterobactin and disrupting the Fe-acquisition process of certain bacteria. However, it has yet to be investigated whether or not Sc is strongly influenced by organic complexation in the water column. Also, as far as we know, there is no biological use of Sc. Potentially the Sc distribution is representative of the side of the Fe cycle that is not driven by Fe's use as a nutrient.

2. Methods

2.1 Sample Collection

Vertical profile samples were analyzed from the 2009 GEOTRACES occupation of the SAFe site in the North Pacific at 30.0°N, 140.0°W (Al, Ga, Sc, Y and La), the 2011 GEOTRACES sampling of the BATS site at 31.8°N, 64.2°W as part of the North Atlantic Zonal Transect (NAZT) (Ga, Sc, Y and La), the 2008 GEOTRACES occupation of the same site (Al), and Station 15 of the 2013 GEOTRACES South Pacific transect at 16.0°S, 104°W (Sc, Y and La). Published profiles of Sc, Y and La (Amakawa et al., 2007; Alibo and Nozaki, 1999; Alibo et al., 1999; Greaves et al., 1990) from other parts of the world ocean were compiled and compared with these locations (Figure 1, discussed in section 3.1).

Samples were collected with the U.S. GEOTRACES carousel of 12L Teflon-coated GO-FLO bottles (Cutter and Bruland, 2012). Samples and reagents were stored in low-density polyethylene bottles that had been rigorously cleaned with the same procedure used for the SAFe and GEOTRACES intercalibration sample bottles (Cutter et al., 2014). Sample bottles were stored filled with weak trace metal grade HCl (~pH 2), and rinsed three times with sample seawater before filling. All samples were filtered through a 0.2 μm polysulfone membrane AcroPak-200® capsule filter, and acidified at sea with the equivalent of 4 mL of 6 N quartz-distilled HCl (Q-HCl) per liter of seawater (to pH 1.7-1.8). Measurements of dissolved Al were made shipboard after the samples had been acidified for at least one hour; all other analyses were performed in the laboratory.

2.2 Multi-element Sample Analysis – Sc, Y, La and Ga

The multi-element method used to analyze samples for Sc, Y, La, and Ga is based upon the method of Biller and Bruland (2012). Briefly, this method involves preconcentration of the metals of interest by extracting a suite of trace metals from buffered seawater samples onto 2 cm columns of Nobias PA1® chelating resin, and then eluting with ~1 mL of quartz distilled 1N HNO_3. The eluent is analyzed with an Element XR Inductively Coupled Plasma Mass Spectrometer (HR ICP-MS) in counting mode (rather than analog or faraday). Scandium and Ga are analyzed in medium resolution, and Y and La are analyzed in low resolution. Scandium was not included in the suite of elements analyzed by Biller and Bruland (2012), nor in the adaptation by Middag et al. (2015), however we report a high recovery (>99%, discussed below) and low detection limit (0.13 pmol/kg) for Sc with this method.

Column blanks and HR ICP-MS system blanks were measured as in Biller and Bruland (2012). For this study, reagent blanks were measured by analyzing low-metal seawater twice normally (rx1) and twice with double the volumes of reagents (rx2). Reagents that were doubled include the Q-HCl originally used to acidify the sample, the buffer to bring the sample up to loading pH, and the In/Lu spike (discussed in supplementary materials). In this way, the rx2 seawater is at the correct pH for loading on the column, and the difference in metal concentrations between rx2 and rx1 is the reagent blank.

Recoveries of the metals were determined by spiking low-metal seawater to make a 5-point standard curve, preconcentrating and analyzing these seawater

standards in the same way as the samples, and comparing the seawater standard curve with one made directly in clean eluent and analyzed in the same HR ICP-MS run. This was performed for every HR ICP-MS run of samples. The recoveries of Sc, Y and La were all >99%, while that of Ga was ~70%. Additional distinctions between the methods used here and those of Biller and Bruland (2012) are discussed in the supplementary materials.

2.3 Aluminum Sample Analysis

Dissolved Al measurements were made using the method of Brown and Bruland (2008), which utilizes in-line preconcentration of dissolved Al onto a commercially available iminodiacetate chelating resin (Toyopearl AF- Chelate 650M®) followed by fluorometric detection of an Al-lumogallion complex. This method has a detection limit of 0.1 nM when preconcentrating 10 mL of sample, and a precision of 2.5% based on replicate analyses of a 5 nmol/L Al sample when preconcentrating 2.5 mL of sample. For sample concentrations above 10 nM such as those concentrations found at the BATS station, sample analysis was carried out with a 2.5 mL preconcentration volume. Blank analysis was performed using acidified MQ water with all the same reagents that was loaded onto the chelating resin at the same volume as the samples being analyzed.

3. Results and Discussion

3.1 Vertical Profiles and Reactivity

At all locations, Y and La concentrations are relatively low in surface waters, increase with depth, and are generally higher in deep-water of older water masses than in those of younger water masses (Figure 1). The most dramatic differences are between the younger deep waters of the North Atlantic BATS station and the older deep waters of the North Pacific SAFe and MNP stations. These are classic characteristics of nutrient-type metals, and this nutrient-like distribution for Y and La has previously been documented (Alibo et al., 1999; de Baar et al., 1985), though never with such wide a range of profiles. Since there are no known biological requirements for Y and La, they are generally thought to be passively adsorbed onto particles rather than actively assimilated (Nozaki, 2001).

Interestingly, the profiles for Y and La do not increase in deep-water concentration in the same pattern. Yttrium appears to increase in deep water concentration at each step we have of the deep-water aging: from the western North Atlantic, to the eastern North Atlantic, the South Pacific, the western North Pacific, and finally to the eastern North Pacific. Lanthanum, however, does not increase in concentration across the North Atlantic to the South Pacific, but does increase in concentration from the South Pacific to the western North Pacific and to the eastern North Pacific. This difference in concentration increase with deep-water age between these two nutrient-type metals could be due to the difference in the ionic radii size: Y is smaller than La (Shannon, 1976), and is predicted to be more strongly complexed

in seawater, and therefore less prone to reversible scavenging, than La (Nozaki, 2001).

Like Y and La, Sc exhibits lower concentrations in the surface than at depth, typical of a nutrient-type metal; however *the deep-water Sc concentration does not increase with aging water masses* (Figure 1). Therefore, the particle reactivity of Sc is high enough that removal of dissolved Sc by scavenging close to balances out the input of dissolved Sc from remineralization. We can conclude from this that Sc is a hybrid-type metal as defined by Bruland and Lohan (2003) and Bruland et al. (2014) that has a short residence time in the deep sea relative to the age of the water mass.

Aluminum and Ga (Figure 2) both show the distribution of classic scavenged-type metals: high concentrations in the surface water and decreasing concentration with age of the deep water. These distributions, which have been thoroughly documented previously (Orians and Bruland, 1985, 1986, 1988a, 1988b; Shiller, 1988; Hydes, 1979), are useful to compare with Sc's distribution to constrain Sc's particle reactivity. Figure 2 clearly shows that Sc is less particle reactive than Al and Ga.

3.2 Residence Times

Table 1 shows 2700-3000 m concentrations of Al, Ga, Sc, Fe, Y and La at the North Atlantic BATS station and the North Pacific SAFe site, Atlantic to Pacific concentration ratios in this depth range for each metal, and estimated deep oceanic residence times. The trivalent ionic size of these metals increases in the order Al<Ga~Fe<Sc<Y<La (Shannon, 1976). With the exception of Fe (discussed below),

this is the same order of decreasing Atlantic to Pacific concentration ratio. Lower Atlantic to Pacific concentration ratios in general correspond with larger ionic size, lesser particle reactivity and therefore longer oceanic residence times. Aluminum exhibits the greatest decrease in deep-water concentration between the Atlantic and the Pacific, followed by Ga, and then Sc and Fe. Y and La have the smallest ratios of the group, indicating longer residence times. Consequently, Sc should have a residence time longer than Al and Ga, but a shorter one than those of Y and La.

The deep oceanic residence time of Al has been estimated to be 100-200 years (Orians and Bruland, 1985), while that of Ga is about 750 years (Orians and Bruland, 1988a). Alibo and Nozaki (1999) estimated the mean oceanic residence time of Y and La to be 2030-5100 years and 650-1630 years, respectively. So, by comparison, the oceanic residence time for dissolved Sc is estimated to be between 750 and 1630 years: on the order of 1000 years. Scandium could therefore offer insights into scavenging similar to Al and Ga but on a longer timescale.

Iron's estimated oceanic residence time is much shorter than would be expected from its Atlantic to Pacific concentration ratio (Table 1). This has caused much discussion in the oceanographic community (e.g. Johnson et al., 1997, Boyd and Ellwood, 2010): how does the concentration of this particle reactive metal remain so similar between the North Atlantic and North Pacific basins? Johnson et al. (1997) suggest that the organic ligands bound to Fe keep some level of Fe in solution protected from scavenging; Boyd and Ellwood (2010) suggest it could be due to regional Fe inputs. It is certainly interesting that despite the general relationship

between residence time, ionic radius, and Atlantic to Pacific concentration ratio, Fe has a residence time close to Al, a trivalent ionic radius close to Ga, and an Atlantic to Pacific concentration ratio similar to Sc. This is yet another example of how complicated the oceanic Fe cycle is.

3.3 A comparison between Sc and Fe

Before going too far into the comparison between Fe and Sc, it should be noted that in addition to Fe's role as an essential micronutrient, there are some important distinctions between Fe and Sc biogeochemistry. First, Fe exhibits redox chemistry while Sc's only oxidation state is 3+. Second, the particulate pools of these two metals in the ocean are very different: Buat-Menard and Chesselet (1979) found particulate Fe to be four orders of magnitude higher in concentration than particulate Sc in the deep Tropical North Atlantic (dissolved concentration differences are more like 1-2 orders of magnitude, table 1). These differences naturally have important impacts on the cycling of Fe and Sc. Despite these differences, the two metals seem to be remarkably similar in their reactivity: they appear to have similar inorganic speciation (Byrne, 2002), a similar Atlantic to Pacific concentration ratio (this work, discussed below), and are able to substitute in some organic complexes (Rogers et al., 1980). Investigating the similarities and differences between Fe and Sc cycling may help us tease out mechanisms of processes in both of their biogeochemical cycles.

The similarity between the deep Atlantic to Pacific ratios for Sc and Fe (1.0 and 0.8, respectively, Table 1) is hypothesized to be due to the similarity of their inorganic speciation (both predominantly Metal-$(OH)_3^0$) and therefore particle

reactivity, as noted in section 1. Since the Atlantic to Pacific concentration ratio is lower for Fe than for Sc, in the balance of scavenging versus remineralization, Fe is closer to being a nutrient-type metal than is Sc. This is not simply due to ionic size differences and corresponding differences in particle reactivity, because Fe^{3+} is slightly smaller than Sc^{3+} (Shannon, 1976), and would therefore in the absence of other variables be closer to scavenged-type than Sc. But there are oceanographic reasons for a lower Fe ratio. Fe is a required micronutrient, and is actively taken up by phytoplankton, so remineralizing biological particles have a greater amount of Fe than they would have purely from inorganic scavenging. Furthermore, a large portion of dissolved Fe in the deep ocean is chelated with organic compounds (Gledhill and Buck, 2012), which could lead to a decrease in its particle reactivity. Scandium may be able to substitute for Fe in these organic complexes, as noted in section 1, but the degree of its possible complexation with organic ligands is unknown. Dissolved Sc is at much lower concentrations in the ocean than dissolved Fe (pmol/kg vs nmol/kg), and while we do not know the solubility of Sc in seawater, there is no reason to suppose that ligands are necessary to keep such a small concentration of Sc in solution. Whether ligands play a significant role in Sc cycling or not, as far as is known there is no biological use of Sc. Oceanic Sc cycling therefore has the potential to help isolate the non-nutrient side of Fe's biogeochemistry, and better constrain the oceanic Fe cycle.

4. Conclusions

Scandium's reactivity is between that of Y and La, its nutrient-type group-mates in Group IIIB, and that of Ga and Al, its scavenged-type group-mates in IIIA. The evidence presented here indicates that Sc is a hybrid-type element that is scavenged from deep water with a residence time on the order of a thousand years. Scandium is a new analyte with distinct particle reactivity from other analytes with inorganically-driven cycling such as Al and Ga. Scandium distributions consequently could offer new insights into scavenging under longer timescales and potentially different particle composition than Al and Ga. Furthermore, Sc's inorganic speciation is similar to that of inorganic Fe, and the change in deep-water concentration from the North Atlantic to the North Pacific is comparable for these two metals. However unlike Fe, Sc has no known biological use, and is not expected to be taken up actively by phytoplankton. The biogeochemistry of Sc in the oceans could therefore be analogous to non-nutrient side of the oceanic Fe cycle.

Acknowledgements

We thank Geoffrey Smith, Greg Cutter, Pete Morton, Jessica Fitzsimmons, Randelle Bundy, and Cheryl Zurbrick for help with sample collection, and Dondra Biller and Russ Flegal for helpful edits, insights, and suggestions on the manuscript. We also thank Rob Franks for his invaluable help with analytical and instrumental challenges, and two anonymous reviewers who helped improve this manuscript. This work was funded by the National Science Foundation under award numbers OCE 0961579 and

OCE 1233502. The data that was used in generating the figures and table in this work can be found in the supplementary materials.

References

Alibo, D. S., and Y. Nozaki (1999), Rare earth elements in seawater: Particle association, shale-normalization, and Ce oxidation, Geochim. Cosmochim. Ac., 63 [3/4], 363-372, doi:10.1016/S0016-7037(98)00279-8.

Alibo, D.S., Y. Nozaki, and C. Jeandel (1999), Indium and yttrium in North Atlantic and Mediterranean waters: comparison to the Pacific data, Geochim. Cosmochim. Ac., 63[13/14], 1991-1999, doi:10.1016/S0016-7037(99)00080-0.

Amakawa, H., M. Nomura, K. Sasaki, Y. Oura, and M. Ebihara (2007), Vertical distribution of scandium in the north central Pacific, Geophys. Res. Lett., 34, LL11606, doi:10.1029/2007GL029903.

Balistrieri, L., P. G. Brewer, and J. W. Murray (1981), Scavenging residence time of trace metals and surface chemistry of sinking particles in the deep ocean, Deep-Sea Res., 28A, 101-121, doi:10.1016/0198-0149(81)90085-6.

Biller, D. V., and K. W. Bruland (2012), Analysis of Mn, Fe, Co, Ni, Cu, Zn, Cd, and Pb in seawater using the Nobias-chelate PA1 resin and magnetic sector inductively coupled plasma mass spectrometry [ICP-MS], Mar. Chem., 130-131, 12-20, doi:10.1016/j.marchem.2011.12.001.

Buat-Menart, P., and R. Chesselet (1979), Variable influence of the atmospheric flux on the trace metal chemistry of oceanic suspended matter, Earth Planet. Sc. Lett., 42(3), 399-411, doi: 10.1016/0012-821X(79)90049-9.

Boyd, P.W., and M.J. Ellwood (2010), The biogeochemical cycle of iron in the ocean, Nat. Geosci., 3, 675-682, doi: 10.1038/ngeo964.

Brown, M.T., and K. W. Bruland (2008), An improved flow-injection analysis method for the determination of dissolved aluminum in seawater, Limnol. Oceanogr. Methods, 6, 87-95, doi:10.4319/lom.2008.6.87.

Bruland, K. W., and Lohan, M. C. (2003), Controls of trace metals in seawater, Treatise on Geochemistry. Elsevier Ltd., V6, [ISBN: 0-08-044341-9], 23-47.

Bruland, K.W., K.J. Orians, and J.P. Cowen (1994), Reactive trace metals in the stratified central North Pacific, Geochim. Cosmochim. Ac., 58(15), 3171-3182, doi: 10.1016/0016-7037(94)90044-2.

Bruland, K.W., R., and M.C. Lohan (2014), Controls of trace metals in seawater, Treatise on Geochemistry (2nd edition), Elsevier, Oxford, [ISBN: ISBN: 978-0-08-098300-4],19-51, doi:10.1016/B978-0-08-095975-7.00602-1.

Byrne, R. H. (2002), Inorganic speciation of dissolved elements in seawater: the influence of pH on concentration ratios, Geochem. Trans., 3(2), 11-16, doi:10.1039/b109732f.

Chen, S. Y., S. Ambe, N. Takematsu, and F. Ambe (1996), Multitracer study on removal mechanism of metal elements from seawater, Analytical Sciences, 12, 1–6, doi:10.2116/analsci.12.1.

Coale, K. H., K. S. Johnson, S. E. Fitzwater, R. M. Gordon, S. Tanner, F. P. Chavez, L. Ferioli, C. Sakamoto, P. Rogers, F. Millero, P. Steinberg, P. Nightingale, D. Cooper, W. P. Cochlan, M. R. Landry, J. Constantiou, G. Rollwagen, A. Trasvina, and R. Kudela (1996), A massive phytoplankton bloom induced by an ecosystem-scale iron fertilization experiment in the equatorial Pacific Ocean, Nature, 383, 495–501, doi:10.1038/383495a0.

Cutter, G. A., and K. W. Bruland (2012), Rapid and noncontaminating sampling system for trace elements in global ocean surveys, Linmol. Oceanogr. Methods, 10, 425- 436, doi:10.4319/lom.2012.10.425.

Cutter, G. A., P. Andersson, L. Codispoti, P. Croot, R. Francois, M. Lohan, H. Obata, and M. R. van der Loeff (2014), Sampling and sample-handling protocols for GEOTRACES cruises, version 2.0, http://www.geotraces.org/images/stories/documents/intercalibration/Cookbook.pdf

de Baar, H. J. W., M. P. Bacon, P. G. Brewer, and K W. Bruland (1985), Rare earth elements in the Pacific and Atlantic Oceans, Geochim. Cosmochim. Ac., 49, 1943-1959, doi:10.1016/0016-7037(85)90089-4.

Fluck, E. and the International Union of Pure and Applied Chemistry (1988), New notations in the periodic table, Pure & Appl. Chem., 60(3), 431-436.

Gledhill M., and C. M. G. van den Berg (1994), Determination of complexation of iron [III] with natural organic complexing ligands in seawater using cathodic stripping voltammetry, Mar. Chem., 47(1), 41-54, doi: 10.1016/0304-4203(94)90012-4.

Gledhill, M., and K. N. Buck (2012), The organic complexation of iron in the marine environment: a review, Front. Microbiol., 3, 69, doi:10.3389/fmicb.2012.00069.

Greaves, M. J., M. Rudnicki, and H. Elderfield (1990), Rare earth elements in the Mediterranean Sea and mixing in the Mediterranean outflow, Earth Planet. Sc. Lett., 103, 169-181, doi:10.1016/0012-821X(91)90158-E.

Hydes, D. J. (1979), Aluminum in seawater: control by inorganic processes, Science, 205, 1260–1262, doi:10.1126/science.205.4412.1260.

Jensen, W. B. (1982), The positions of lanthanum (actinium) and lutetium (lawrencium) in the periodic table, J. Chem. Educ., 59(8), 634-636, doi:10.1021/ed059p634.

Johnson, K.S., R.M. Gordon, and K.H. Coale (1997), What controls dissolved iron concentrations in the world ocean?, Mar. Chem., 57, 137-161, doi:10.1016/S0304-4203(97)00043-1.

Lavelle, L. (2008), Lanthanum (La) and actinium (Ac) should remain in the d-block, Journal of Chemical Education, 85(11), 1482, doi:10.1021/ed085p1482.

Lohan, M. C., A. M. Aguilar-Islas, R. P. Franks, and K. W. Bruland (2005), Determination of iron and copper in seawater at pH 1.7 with a new commercially available chelating resin NTA Superflow, Anal. Chim. Acta., 530, 121–129, doi:10.1016/j.aca.2004.09.005.

Martin, J. H., R. M. Gordon, S. E. Fitzwater, W. W. Broenkow (1989), Vertex: phytoplankton/iron studies in the Gulf of Alaska, Deep-Sea Res. I, 36, 649–680, doi:10.1016/0198-0149(89)90144-1.

Middag, R., R. Séférian, T. M. Conway, S. G. John, K. W. Bruland, and H. J. W. de Baar (2015), Intercomparison of dissolved trace elements at the Bermuda Atlantic Time Series station, Mar. Chem., 177(3), 476-489, doi:10.1016/j.marchem.2015.06.014.

Moore, J. K., S. C. Doney, D. M. Glover, I. Y. Fung (2002), Iron cycling and nutrient-limitation patterns in surface waters of the World Ocean, Deep-Sea Res. II, 49, 463-507, doi:10.1016/S0967-0645(01)00109-6.

Nozaki, Y. (2001), Rare earth elements and their isotopes, Encyclopedia of Ocean Sciences, vol. 4, edited by J. Steele, S. Thorpe, and K. K. Turekian, pp. 2354–2366, Academic Press, London.

Orians, K. J. and K. W. Bruland (1985), Dissolved aluminum in the central North Pacific, Nature, 316 (1), 427-429, doi:10.1038/316427a0.

Orians K. J. and K. W. Bruland (1986), The biogeochemistry of aluminum in the Pacific Ocean, Earth Planet. Sc. Lett., 78, 397–410, doi:10.1016/0012-821X(86)90006-3.

Orians, K. J., and K. W. Bruland (1988a), Dissolved gallium in the open ocean, Nature, 332(21), 717-719, doi:10.1038/332717a0.

Orians, K. J., and K. W. Bruland (1988b), The marine geochemistry of dissolved gallium: A comparison with dissolved aluminum, Geochim. Cosmochim. Ac., 52, 2955-2962, doi:10.1016/0016-7037(88)90160-3.

Rogers, H.J., C. Synge, and V.E. Woods (1980), Antibacterial effect of scandium and indium complexes of enterochelin on Klebsiella pneumoniae, Antimicrob. Agents Ch., 18(1), 63-68, doi: 10.1128/AAC.18.1.63.

Rue, E. L., and K. W. Bruland (1995). Complexation of iron[III] by natural organic ligands as determined by a new competitive equilibration/adsorptive cathodic stripping voltammetry method, Mar. Chem., 50, doi:117–13910.1016/0304-4203[95]00031-L.

Rue, E. L. and K. W. Bruland (1997), The role of organic complexation on ambient iron chemistry in the Equatorial Pacific Ocean and the response of a mesoscale iron addition experiment, Limnol. Oceanogr.. 42, doi:10.4319/lo.1997.42.5.0901.

Shannon, R.D. (1976), Revised effective ionic radii and systematic studies of interatomic distances in halides and chalcogenides, Acta. Crystallogr. A., A32, 751-767, doi:10.1107/S0567739476001551.

Shiller, A.M. (1988), Enrichment of dissolved gallium relative to aluminum in natural waters, Geochim. Cosmochim. Ac., 52, 1879-1882, doi:10.1016/0016-7037(88)90011-7.

Taylor, S. R., S. M. McLennan, and M. T. McCulloch (1983), Geochemistry of loess, continental crustal composition and crustal ages, Geochim. Cosmochim. Acta., 47, 1897–1905, doi:10.1016/0016-7037(83)90206-5.

van den Berg, C. M. G. (1995), Evidence for organic complexation of iron in seawater, Mar. Chem., 50(1-4), 139-157, doi:10.1016/0304-4203(95)00032-M.

Wu, J., and G. W. Luther III (1995), Complexation of iron[III] by natural organic ligands in the Northwest Atlantic Ocean by a competitive ligand equilibration

method and a kinetic approach, Mar. Chem., 50(1-4), 159-177, doi:10.1016/0304-4203(95)00033-N.

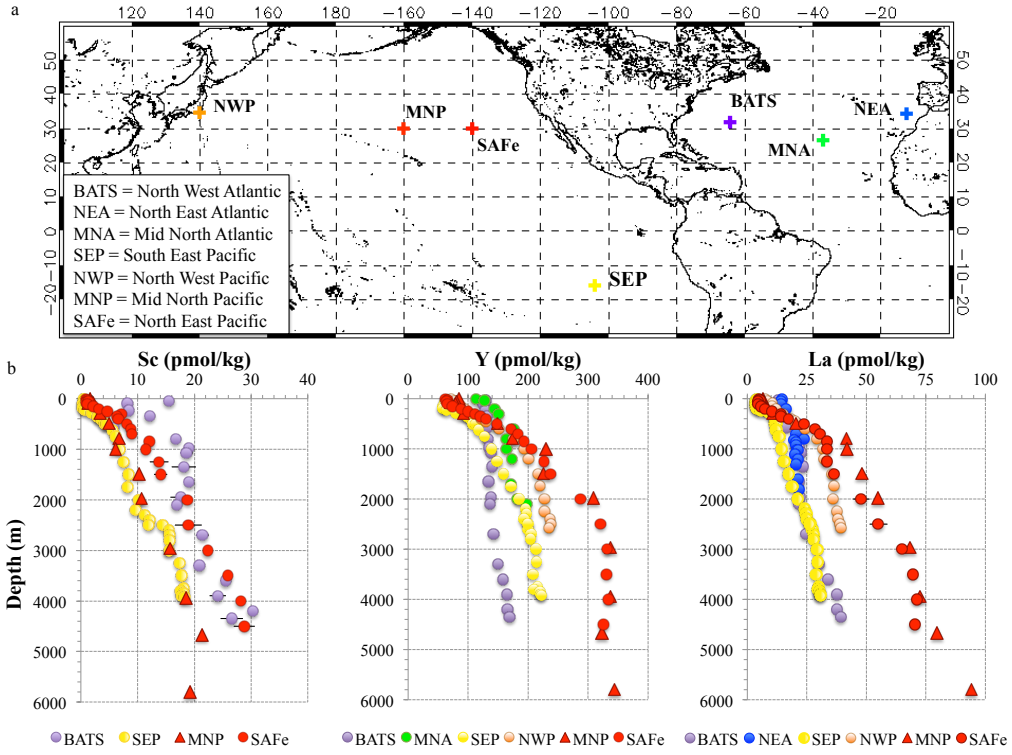

Figure 1: Depth profiles of dissolved Sc, Y and La from diverse regions of the world ocean. Colors roughly correspond to the age of the deep water: cooler colors (purple, blue) represent younger waters and warmer colors (red, orange) represent older waters. The colors of the location markers in 1a correspond with the colors of the data points in 1b. Error bars show one standard deviation away from the mean of four replicates for BATS, and two replicates for SAFe. South East Pacific (SEP) data was run in singlicate. MNA data from Alibo et al. (1999), NEA data from Greaves et al. (1990), NWP data from Alibo and Nozaki (1999), and MNP data from Amakawa et al. (2007). Map plotted with Interactive Data Language®, a product of Exelis Visual Information Solutions, Inc., a subsidiary of Harris Corporation (Exelis VIS).

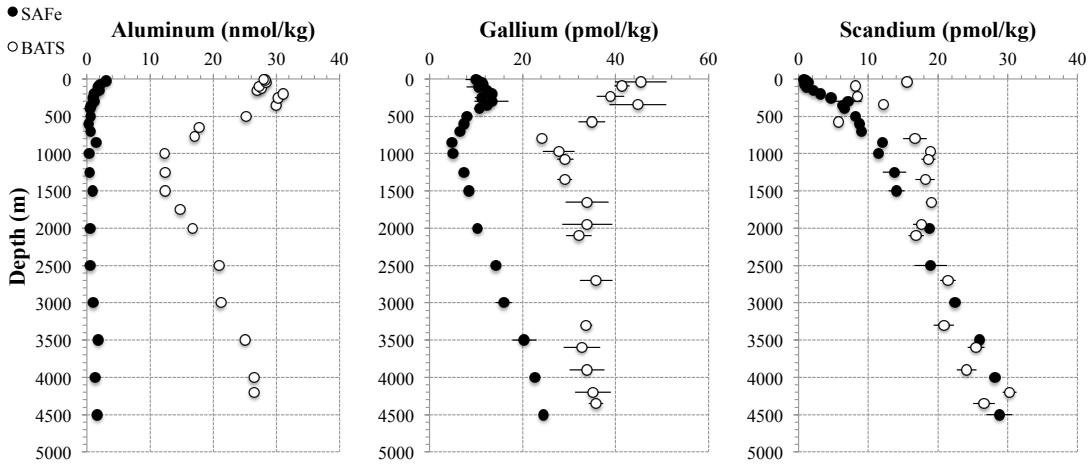

Figure 2: Al, Ga and Sc depth profiles in the North Atlantic at the BATS stations and in the North Pacific at the SAFe site. Al shows the greatest percent difference in deep water concentration between the Atlantic and the Pacific, followed by Ga and then Sc. Error bars show one standard deviation away from the mean of four replicates for BATS Ga and Sc profiles, and two replicates for SAFe Ga and Sc profiles. Al is reported in singlicate.

	Units	Atlantic (BATS)	Pacific (SAFe)	Atlantic to Pacific ratio	Deep Oceanic Residence Time (years)
Aluminum	nmol/kg	21.2	0.97	21.9	100-200
Gallium	pmol/kg	35.8	16	2.2	750
Scandium	pmol/kg	21.4	22.4	1.0	~1000
Iron	nmol/kg	0.49	0.63	0.8	70-200
Yttrium	pmol/kg	130	332	0.4	2030-5100
Lanthanum	pmol/kg	21.5	64.7	0.3	650-1630

Table 1: Concentrations and ratios of dissolved Al, Ga, Sc, Fe, Y and La at 2700-3000 m in the North Atlantic and North Pacific (BATS and SAFe site, respectively), and estimated deep oceanic residence times for each metal. Higher Atlantic to Pacific ratios generally correspond with shorter oceanic residence times. SAFe data is from the GEOTRACES 2009 occupation at 3000 m, BATS Al and Fe data is from the 2008 GEOTRACES occupation at 3000 m, and BATS Ga, Sc, Y and La data is from the 2011 GEOTRACES occupation at 2700 m. Iron data is from Biller and Bruland (2012). Residences times are from Orians and Bruland (1985) (Al), Orians and Bruland (1988a) (Ga), inferred in this work (Sc), Bruland et al. (1994) and Johnson et al. (1997) (Fe), and Alibo and Nozaki (1999) (Y and La).

CHAPTER 2: DISSOLVED SCANDIUM, YTTRIUM, AND LANTHANUM IN THE SURFACE WATERS OF THE NORTH ATLANTIC: POTENTIAL USE AS AN INDICATOR OF SCAVENGING INTENSITY

Claire E. Parker, Rachel U. Shelley, William M. Landing, Kenneth W. Bruland

Abstract

Recent work (Amakawa et al., 2007; Parker et al., accepted) has begun to elucidate the biogeochemical cycling of scandium (Sc) in the open ocean, but so far no surface distribution data has been reported of dissolved Sc, and no basin-scale surface distributions have been reported of yttrium (Y) or lanthanum (La). This work presents basin-wide surface Sc, Y and La data in a section across the North Atlantic subtropical gyre (GEOTRACES GA-03) and investigates the potential utility of the distributions as an indicator of surface ocean particle scavenging. This work shows that the surface distribution of Sc in the North Atlantic correlates with the shape of the gyre as calculated by isotherm depth, suggesting that the Sc concentration is drawn down by elevated particle flux at the gyre boundaries, and therefore Sc removal could be used as an indicator of scavenging intensity. In order to account for variable input of Sc to the surface ocean, we propose normalizing the Sc distribution to those of Y or La, which increases the correlation with the shape of the gyre. We propose that the variation in dissolved Y/Sc and La/Sc ratios is due to Sc removal by scavenging, and is therefore an indicator of scavenging intensity. Surface samples

from the North Atlantic show higher Y/Sc and La/Sc ratios in regions with expected higher export production.

1. Introduction

Recent investigation has shown that scandium (Sc), yttrium (Y) and lanthanum (La), three of the four elements generally considered to be in Group IIIB of the periodic table, have contrasting reactivity in the ocean (Parker et al., accepted): Sc is a hybrid-type metal, with a roughly-equal balance between particle scavenging and remineralization governing its distribution in the deep sea (Parker et al., accepted), while Y and La are classic nutrient-type metals increasing in deep-water concentration with age of the deep water (de Baar et al., 1985; Alibo et al., 1999).

Investigations of Sc distributions and the potential use of this contrasting reactivity between Sc and the other two metals are in early stages. There are only two modern publications with depth profiles of Sc (Amakawa et al., 2007; Parker et al., accepted), resulting in a total of four depth profiles globally, and no surface ocean transect data for dissolved Sc has been reported to date. There has been a greater degree of investigation into the biogeochemical cycling of Y and La (e.g. de Baar et al., 1985; Greaves et al., 1990; Alibo et al., 1999; Alibo and Nozaki, 1999; Nozaki, 2001), but to the authors' knowledge this does not include any basin-scale surface distributions. This work presents surface transect concentration data of Sc, Y, and La in the North Atlantic and investigates the potential of using the contrasting reactivity between Sc and the other two metals as an indicator of surface-ocean scavenging intensity.

Other scavenging indicators such as Al, Ga, $^{231}Pa/^{230}Th$, ^{234}Th, ^{228}Th, and $^{210}Po/^{210}Pb$ have been valuable in investigating scavenging throughout the water column (e.g. Bacon and Anderson, 1982; Henderson and Slowey, 2000; Savoye et al., 2006; Rutgers v.d. Loeff and Geibert, 2008). Each indicator offers specific insights into scavenging timescales or particle composition. The Al distribution has also been used to constrain modeled atmospheric dust deposition (Measures and Brown, 1995). Since Sc is less particle reactive than Al and Ga (Parker et al., accepted), Sc could provide insights into dust deposition and scavenging on longer timescales than Al and Ga.

In order to use Sc removal in the surface ocean as an indicator of scavenging, it is necessary to account for variable Sc input into the surface ocean. Where atmospheric deposition is the main source, we propose that it may be possible to do so by normalizing the surface dissolved Sc distribution to those of Y or La. Ratios of Sc, Y, Th and the lanthanides have been used in studies to identify the provenance of dust (e.g. Pease and Tchakerian, 2002), so it follows that if dust from one provenance is the main source of Sc, Y and La to the surface ocean, they must be input to the surface ocean in roughly constant ratios. Any deviation from those ratios in the dissolved metals would then be a result of differential scavenging of the elements. The North Atlantic is an extreme in terms of degree of mineral dust deposition into the surface ocean. Saharan dust carried by the westerly winds results in some of the highest amounts of dust deposition globally to be deposited into the low- and mid-latitude surface North Atlantic (e.g. Prospero and Carlson, 1972; Jickells et al., 2005).

In this location, we are confident that atmospheric dust is the main source of Sc, Y and La to the surface ocean.

This work presents high resolution surface transect data for dissolved concentrations of Sc, Y and La, significantly adding to the pool of published data on dissolved Sc distributions, and investigates the possibility that removal of Sc by scavenging, as observed by the resulting offset in the dissolved Y/Sc and La/Sc ratios, could give new insights into the relative degree of scavenging across a region.

2. Methods

2.1 Dissolved Sample Collection and Analysis

Surface samples were analyzed from the U.S. GEOTRACES North Atlantic Zonal Transect (NAZT) cruise which went from Woods Hole, MA, past Bermuda, and eastward across the North Atlantic Gyre to Cape Verde at about 17°N (Figure 1). Surface samples were taken and analyzed at a higher frequency than the vertical profile stations labeled on Figure 1. Figure 2 shows the estimated location of the cruise track overlaid on a map of modeled annual export production, reproduced from Falkowski et al. (1998). The cruise track covered a large range of annual mean export production, and therefore is beneficial to use for investigating trace metal scavenging and its influence by export production of biological particles.

Samples were obtained with a surface "GeoFish" sampling system (Bruland et al., 2005). Samples that corresponded with a station depth profile were filtered subsequently through 0.45 μm and then 0.2 μm Osmonics® cartridge filters.

Additional surface samples were taken between stations and were filtered through a 0.2 μm polysulfone membrane AcroPak-200. No difference was observed between the two filtration methods. Reagent and sample bottles were low-density polyethylene, and were rigorously acid cleaned prior to use following the procedure in the GEOTRACES cookbook (Cutter et al., 2014). Bottles were rinsed with sample three times before filling, and all samples were acidified at sea with the equivalent of 4 mL of 6 N quartz-distilled HCl per liter of seawater.

The multi-element dissolved method that was used for analyzing Sc, Y, and La concentrations was adapted from Biller and Bruland (2012). Briefly, this method involves buffering the sample to a specific pH (4.5, 6.0 or 8.3 for this work, all of which work equally well for the three metals of interest), loading the sample onto 2 cm columns of Nobias-chelate PA1 resin, eluting with a small volume of quartz-distilled 1N HNO_3, and analyzing for Sc, Y and La with a High Resolution Inductively Coupled Plasma Mass Spectrometer (HR ICP-MS; Thermo Element XR). Deviations from the method are described in Parker et al. (accepted). Scandium, Y and La are all recovered at >99% using these methods.

2.2 Aerosol Sample Collection and Analysis Methods

Aerosol total suspended particulate samples (n=39) were collected along the NAZT transect. They were collected on Whatman 41 mixed cellulose ester filter discs (47 mm diameter) using a high-volume Total Suspended Particulates TSP sampler (model 5170-BL, Tisch Environmental), at a flow rate of ~1 m^3/min (Shelley et al., 2015). A specially adapted filter holder was manufactured in-house at Florida State

University to hold twelve replicate filter discs. The filters were digested in tightly capped Teflon vials at 150 °C using sequential additions of ultra-high purity HNO_3, and HNO_3 + HF at a ratio of 5:1 (Morton et al., 2013). Separate filters were leached using an "instantaneous" flow-through technique, in which the filter is placed on top of a GN6 (Pall Inc.) backing filter (0.45 mm cut-off; cellulose esters) in a polysulfone filter holder (Nalgene) and 100 mL of ultra-high purity (UHP) water (18 MΩ cm^{-1}) is pulled through the filter within 10 seconds by applying a vacuum (Buck, et al., 2006). Trace elements in leachate solutions were determined by HR ICP-MS (Element 2, Thermo) at the National High Magnetic Field Laboratory at Florida State University. For the remainder of this work, the trace elements that were leached from these aerosols with UHP water will be referred to as DI soluble aerosols.

3. Results and Discussion

3.1 North Atlantic Surface Distributions

The surface distributions of dissolved Sc, Y and La across the North Atlantic show several different trends (Figure 3). Concentrations of Sc are low on the western edge of the basin, they rise rapidly within the oligotrophic central gyre and plateau over 58-68°W before steadily decreasing toward the more productive eastern boundary (Figure 3a). The Y distribution also shows a gradual decrease in concentration moving eastward, but near the western edge of the basin there is a slight increase in Y concentration (Figure 3b). Lanthanum shows the same increase in concentration in the west, but does not show the general decrease in concentration

moving eastward across the basin and contrastingly rises in concentration on the eastern side of the basin (Figure 3c). On the western side of the basin, the drop in dissolved Sc and the increase in Y and La correspond with the introduction of a different water mass with distinct chemical characteristics (Figure 3d). The northern boundary of the Gulf Stream is often accepted to be where the 15°C isotherm is at 200 m, as proposed by Fuglister and Voorhis (1965). Figure 4a indicates that the 15°C isotherm is at 200 m at 67-68°W, so the rapid decrease in dissolved Sc and increase in Y and La concentrations near shore likely corresponds with crossing the Gulf Stream's strong northern boundary and leaving its relatively warm and saline waters. Traditional scavenging indicators Al, Ti, ^{230}Th, ^{231}Pa, and ^{232}Th all show maxima around 50°W (Mawji et al., 2015), while Sc highlights a feature at 58-68°W, so Sc tells a different story and could provide unique insights into scavenging behavior.

The surface Sc distribution across the North Atlantic is strikingly similar to the shape of the gyre (Figure 4). Both sea surface height and Sc concentration have a maximum on the western side of the gyre with a steeper gradient down to the western edge and a more gradual one to the eastern boundary. A contour plot of temperature (Figure 4a), indicating the location of the western warm pool and the degree of thermocline shoaling, shows a similar pattern to the surface Sc concentration (Figure 4b) across the transect: the maximum gradient in the thermocline occurs at 68-70°W, precisely the location of the maximum increase in surface Sc concentration. The surface Sc concentration is consistent through the deepest part of the thermocline (58-

68°W), and then both Sc and the thermocline have a gradual change moving eastward. This correlation between the thermocline depth and the surface Sc concentration is illustrated by Figure 4c, where surface Sc concentration is plotted against the depth of the 17°C isotherm across the transect (at locations where we have data for both parameters; unfortunately there were no paired samples at the far western end of the transect with steep gradients). There is a good correlation between these parameters (R^2=0.91, Figure 4c).

This correlation between the surface Sc distribution and the shape of the gyre could be due to the corresponding nutriclines. Where the nutriclines are closer to the surface, over time there could be enhanced enrichment of nutrients to the surface waters and greater export production that in turn would lead to intensified Sc scavenging and removal of surface dissolved Sc. Figure 2 shows modeled annual mean export production globally, and it is clear that generally export production also corresponds with the shape of the gyre.

3.2 Potential Use for La/Sc and Y/Sc Ratios

This surface Sc distribution is intriguing and suggests that surface Sc concentration may relate to export production, but in order to be able to use dissolved Sc as an indicator of scavenging, it is important to be able to account for variable input of Sc to the surface ocean. Figure 5 shows that there is variation in the DI soluble Sc aerosol input over the North Atlantic transect. The highest DI aerosol input of Sc occurs on the eastern boundary of the basin, where the dissolved Sc is actually at its lowest concentration. Increased removal of dissolved Sc must be occurring on

the eastern boundary, more than balancing out the increased aerosol dust input. If this increased Sc input is not taken into account, the Sc removal in that part of the transect would be underestimated.

If Sc, Y and La are input to the surface ocean in fairly constant ratios, the surface Sc distribution can be normalized to Sc input with Y or La, and this will take into account the variable input of Sc across the basin. Input of Sc, Y and La to the surface North Atlantic Ocean is likely dominated by mineral dust from the Sahara. Figure 6a shows molar ratios of La/Sc in DI soluble aerosols and dissolved surface samples along the transect, and the variation in the aerosol input is indeed minimal compared with the dissolved ratio. Therefore the variation of the dissolved ratio across the transect must be due to processes occurring in the seawater. Because the reactivity of Sc is so much higher than that of La (Parker et al., accepted), it is assumed that the variability in the dissolved La/Sc ratio is driven by Sc scavenging. Consequently, higher dissolved La/Sc ratios are indicative of greater degrees of Sc scavenging.

Without having DI soluble aerosol data for Y, we cannot be sure whether the input ratio of Y/Sc varies minimally compared with the dissolved ratio. However, the dissolved Y/Sc distribution (Figure 6b) is strongly correlated with the La/Sc distribution ($R^2 = 0.99$, Figure 6c), which suggests that Y could be used as an alternative to La. Y/Sc ratios could be more useful than La/Sc ratios because Y is almost an order of magnitude higher in surface concentration than La, so reproducible surface Y values are easier to obtain.

Surface Y/Sc and La/Sc ratios are higher in the boundary regions of the North Atlantic gyre (Figures 6a and b), indicating depleted Sc from increased scavenging in these regions. This makes sense because gyre boundaries are more productive and closer to coastal/shelf inputs of lithogenic material, both of which elevate particle flux and could contribute to increased Sc scavenging intensity. Quantitatively, the Y/Sc and La/Sc ratios also correlate well with the thermocline (correlation with 13°C isotherm R^2=0.97 and 0.95, respectively, Figure 7). Interestingly, the correlations between the isotherm depth and the Y/Sc and La/Sc ratios are strongest for 10-14°C while the correlation with Sc concentrations is highest at 17°C (Figure 8). Deeper isotherms represent a more permanent thermocline, which suggests that normalizing the Sc distribution to Y and La makes the distribution relevant on a longer timescale. The correlation with an isotherm depth is stronger for both Y/Sc and La/Sc than for Sc alone, which supports normalizing the Sc distribution to Y or La to make it more oceanographically relevant.

Why should the depth of an isotherm relate to the concentrations or ratios of metals on the surface? As mentioned briefly above, we propose that it is the corresponding nutriclines that cause this correlation. Where nutriclines are closer to the surface, over time there is enhanced nutrient enrichment to the surface, which leads to greater export production and a greater degree of removal of Sc due to increased scavenging intensity. From this hypothesis, it follows that Sc removal may correlate with export production. From Figure 2, which is a modeled yearly average of export production globally, it is clear that greater degrees of export production

occur at the gyre boundaries, and that the western warm pools have the lowest degrees of export production. This distribution of modeled annual mean export production qualitatively correlates with the shape of the gyre and the distributions of surface dissolved Y/Sc and La/Sc ratios in the North Atlantic.

4. Conclusions

Surface Sc distributions, normalized to Sc input by surface Y or La distributions, have the potential to serve as a new indicator of scavenging intensity. In the North Atlantic, where atmospheric deposition is likely the main source of these three metals to the surface ocean, dissolved surface samples have an order of magnitude greater variability of the La/Sc molar ratio than DI-soluble aerosols fraction, indicating that the dissolved distribution is due to processes occurring in the seawater. Since Sc is significantly more particle reactive than Y and La, we suggest that the Y/Sc and La/Sc distributions reflect Sc drawdown by particle scavenging, and so give an indication of the relative degree of scavenging in a region. The surface La/Sc and Y/Sc distributions correlate well with the depth of the thermocline and the shape of the North Atlantic gyre. We propose that this is due to Sc removal over time in regions with shoaled nutriclines and higher export production, and that therefore surface La/Sc and Y/Sc ratios could be used as indicators of export production.

Future studies crossing other oligotrophic gyres would be useful in investigating whether this correlation holds in regions with lower mineral dust input. It would also be useful to study how particle type affects Sc scavenging: laboratory tests observing Sc scavenging under different particle types would test this directly.

Finally, it would be instructive to look at Sc, Y and La ratios in sediment trap material in order to see what ratios are being removed from the water column, and by what type of particle.

Acknowledgements

The authors thank the captain and crew of the R/V Knorr, the chief scientists Ed Boyle and Greg Cutter, Geoffrey Smith for sample collection, Rob Franks for invaluable instrumental assistance, and Russ Flegal and Dondra Biller for helpful insights and suggestions on the manuscript. This work was funded by the National Science Foundation through award numbers OCE 0961579 and OCE 1233502.

References

Alibo, D. S., and Y. Nozaki (1999), Rare earth elements in seawater: Particle association, shale-normalization, and Ce oxidation, Geochim. Cosmochim. Ac., 63 [3/4], 363-372, doi:10.1016/S0016-7037(98)00279-8.

Alibo, D.S., Y. Nozaki, and C. Jeandel (1999), Indium and yttrium in North Atlantic and Mediterranean waters: comparison to the Pacific data, Geochim. Cosmochim. Ac., 63[13/14], 1991-1999, doi:10.1016/S0016-7037(99)00080-0.

Amakawa, H., M. Nomura, K. Sasaki, Y. Oura, and M. Ebihara (2007), Vertical distribution of scandium in the north central Pacific, Geophys. Res. Lett., 34, LL11606, doi:10.1029/2007GL029903.

Bacon, M.P., and R.F. Anderson (1982), Distribution of thorium isotopes between dissolved and particulate forms in the deep sea, J. Geophys. Res., 87, 2045-2056, doi:10.1029/JC087iC03p02045.

Biller, D. V., and K. W. Bruland (2012), Analysis of Mn, Fe, Co, Ni, Cu, Zn, Cd, and Pb in seawater using the Nobias-chelate PA1 resin and magnetic sector inductively coupled plasma mass spectrometry [ICP-MS], Mar. Chem., 130-131, 12-20, doi:10.1016/j.marchem.2011.12.001.

Bruland, K.W., E.L. Rue, G.J. Smith, and G.R. DiTullio (2005), Iron, macronutrients and diatom blooms in the Peru upwelling regime: brown and blue waters off Peru, Mar. Chem., 93, 81-103, doi: 10.1016/j.marchem.2004.06.011.

Buck C.S., W.M. Landing, J.A. Resing, and G.T. Lebon (2006), Aerosol iron and aluminum solubility in the northwest Pacific Ocean: Results from the 2002 IOC cruise, Geochem. Geophy. Geosy., 7[4], doi: 10.1029/2005GC000977.

Cutter, G.A., P. Andersson, L. Codispoti, P. Croot, R. Francois, M. Lohan, H. Obata, and M. R. van der Loeff (2014), Sampling and sample-handling protocols for GEOTRACES cruises, version 2.0, http://www.geotraces.org/images/stories/documents/intercalibration/Cookbook.pdf.

de Baar, H.J.W., M.P. Bacon, P.G. Brewer, and K.W. Bruland (1985), Rare earth elements in the Pacific and Atlantic Oceans, Geochim. Cosmochim. Ac., 49, 1943-1959, doi:10.1016/0016-7037(85)90089-4.

Falkowski, P.G, R.T. Barber, and V. Smetocek (1998), Biogeochemical controls and feedbacks in organic primary production, Science, 281, 200-206, doi: 10.1126/science.281.5374.200.

Fuglister, F.C., and A.D. Voorhis (1965), A new method of tracking the Gulf Stream, Limnol. Oceangr., 10, R115-R124, doi:10.4319/lo.1965.10.suppl2.r115.

Greaves, M.J., M. Rudnicki, and H. Elderfield (1990), Rare earth elements in the Mediterranean Sea and mixing in the Mediterranean outflow, Earth Planet. Sc. Lett., 103, 169-181, doi:10.1016/0012-821X(91)90158-E.

Henderson, G.M., and N.C. Slowey (2000), Evidence from U-Th dating against Northern Hemisphere forcing of the penultimate deglaciation, Nature, 404, 61-66, doi: 10.1038/35003541.

Jickells, T.D., Z.S. An, K.K. Anderson, A.R. Baker, G. Bergametti, N. Brooks, J.J. Cao, P.W. Boyd, K.A. Hunter, H. Kawahata, N. Kubliay, J. laRoche, P.S. Liss, N. Mahowald, J.M. Prospero, A.J. Ridgwell, I. Tegen, R. Torres (2005), Global iron connections between desert dust, ocean biogeochemistry, and climate, Science, 308, 67-71, 10.1126/science.1105959.

Mawji, E., et al., The GEOTRACES Intermediate Data Product 2014, Mar. Chem. (2015), http://dx.doi.org/10.1016/j.marchem.2015.04.005.

Measures, C.I. and E. Brown (1995), Estimating dust input to the Atlantic Ocean using surface aluminium concentrations, The Impact of Desert Dust Across the Mediterranean, 301-311, doi:10.1007/978-94-017-3354-0_30.

Morton, P.L., W.M. Landing, S.-C. Hsu, A. Milne, A.M. Aguilar-Islas, A.R. Baker, A.R. Bowie, C.S. Buck, Y. Gao, S. Gichuki, M.G. Hastings, M. Hatta, A.M. Johansen, R. Losno, C. Mead, M.D. Patey, G. Swarr, A. Vandermark, and L.M. Zamora (2013), Methods for the sampling and analysis of marine aerosols: results from the 2008 GEOTRACES aerosol intercalibration experiment, Limnol. Oceanogr.-Meth., 11, 62-78, doi: 10.4319/lom.2013.11.62.

Nozaki, Y. (2001), Rare earth elements and their isotopes, Encyclopedia of Ocean Sciences, vol. 4, edited by J. Steele, S. Thorpe, and K. K. Turekian, pp. 2354–2366, Academic Press, London.

Parker, C.E., M.T. Brown, and K.W. Bruland (accepted), Scandium in the open ocean: A comparison with other group 3 trivalent metals, Geophys. Res. Lett., doi:10.1002/2016GL067827.

Pease, P.P., and V.P. Tchakerian (2002), Composition and sources of sand in the Wahiba Sand Sea, Sultanate of Oman, Ann. Assoc. Am. Geogr., 92, 416–434, doi: 10.1111/1467-8306.00297.

Prospero, J.M., and T.N. Carlson (1972), Vertical and areal distribution of Saharan dust over the Western Equatorial North Atlantic Ocean, J. Geophys. Res., 77[27], 5255-5265, doi: 10.1029/JC077i027p05255.

Rutgers van der Loeff, M.M., and W. Geibert (2008), U- and Th-series nuclides as tracers of particle dynamics, scavenging and biogeochemical cycles in the oceans, in U-Th Series Nuclides in Aquatic Systems, 227–268, Elsevier, doi:10.1016/S1569-4860(07)00007-1.

Savoye, N., C. Benitez-Nelson, A.B. Burd, J.K. Cochran, M. Charette, K.O. Buesseler, G.A. Jackson, M. Roy-Barman, S. Schmidt, and M. Elskens (2006), 234^{Th} sorption and export models in the water column: a review, Mar. Chem., 100, 234-249, doi:10.1016/j.marchem.2005.10.014.

Shelley, R.U., P.L. Morton, and W.M. Landing (2015), Elemental ratios and enrichment factors in aerosols from the US-GEOTRACES North Atlantic transects, Deep-Sea Res. Pt. II, 116, 262-272, doi: 10.1016/j.dsr2.2014.12.005.

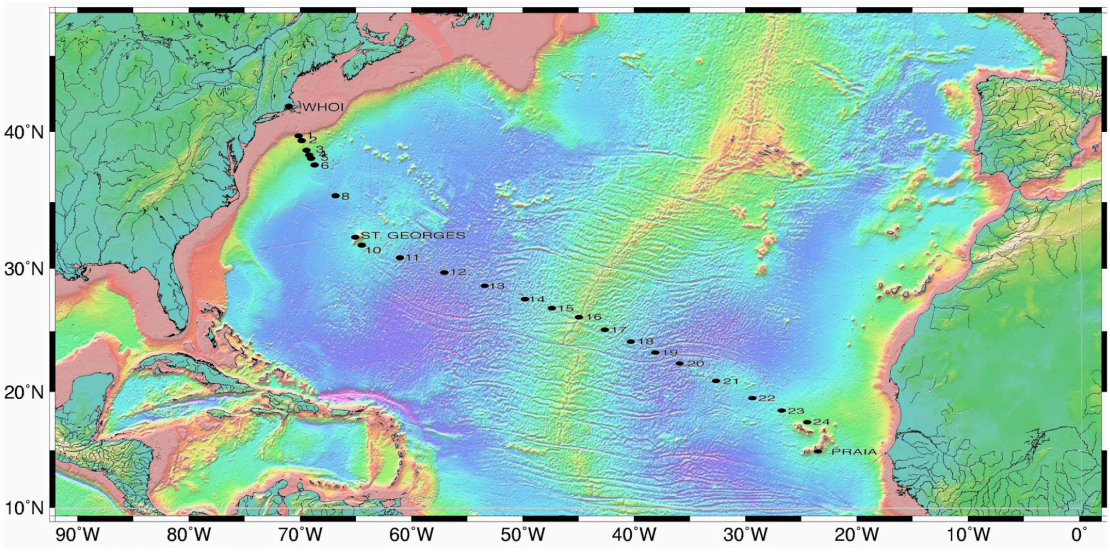

Figure 1: Cruise track for the 2011 North Atlantic GEOTRACES transect from Woods Hole, MA to Praia, Cape Verde. Surface data from this cruise is reported from samples taken along the cruise track, at and between the labeled stations.

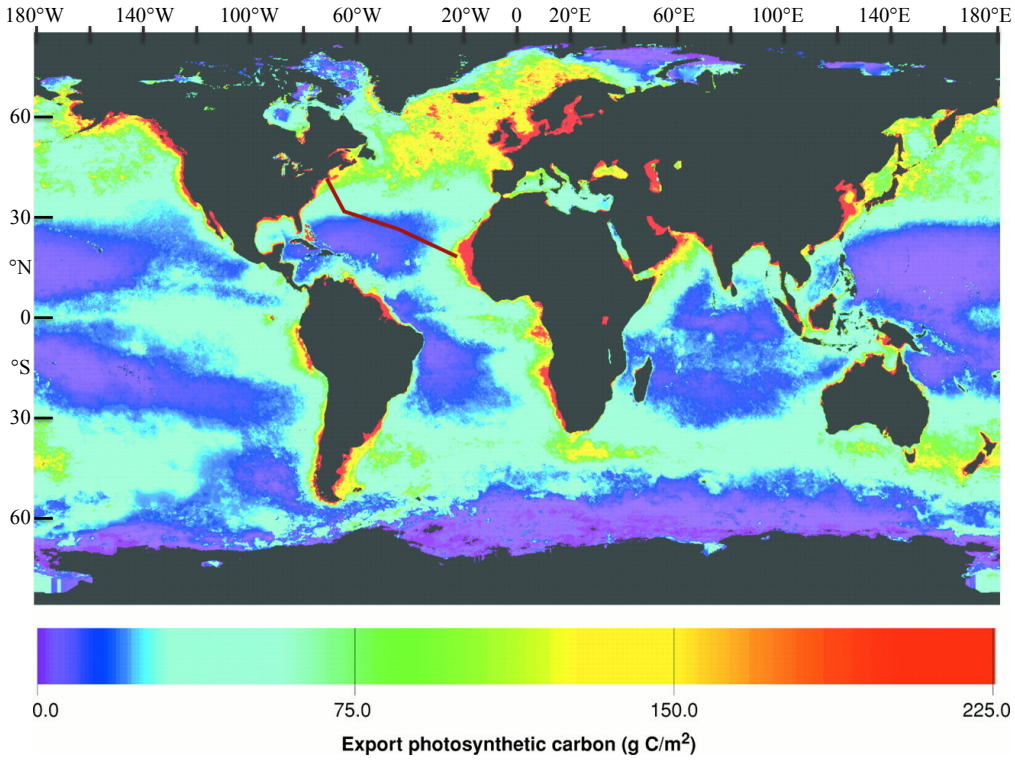

Figure 2: Reproduced with permission from Falkowski et al. (1998), this figure shows modeled annual mean export production globally. Estimated cruise track for the North Atlantic cruise is overlaid. The cruise track crosses the oligotrophic gyre and includes a wide range of export production.

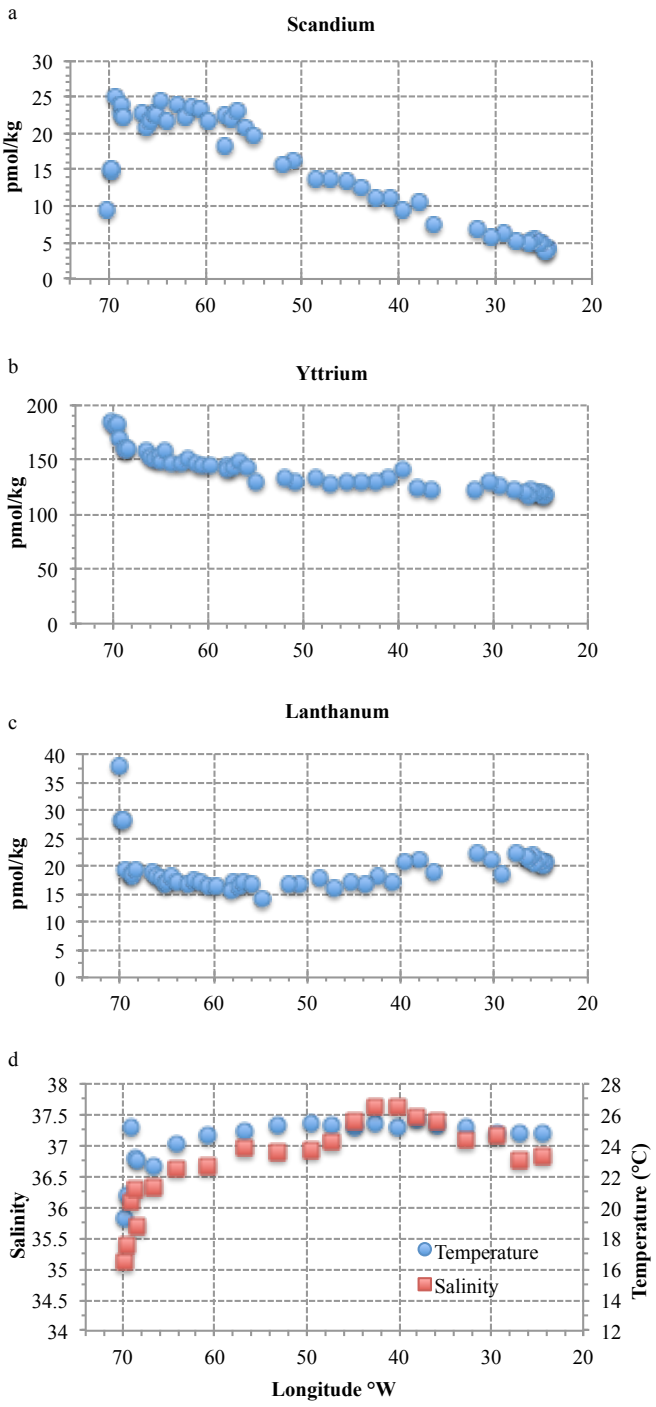

Figure 3 (a), (b) and (c): Surface distributions dissolved Sc, Y, and La, respectively, along the 2011 North Atlantic GEOTRACES transect. (d): Surface temperature and salinity along the same transect. The rapid change in concentrations of all metals at ~67-70°W corresponds with entering the warmer, more highly saline waters of the Gulf Stream.

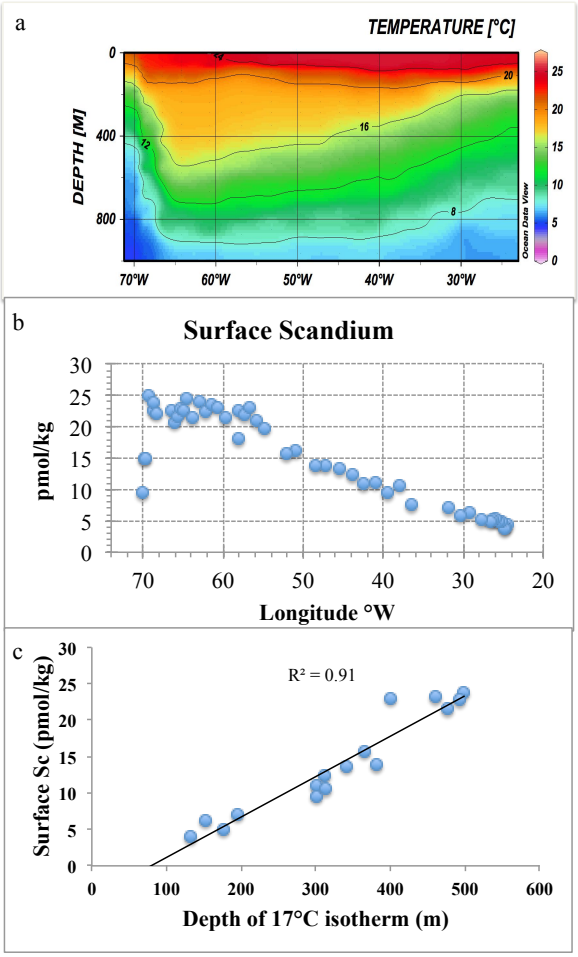

Figure 4 (a): contour plot of temperature to 1000m along the North Atlantic Transect (b): dissolved Sc in the surface of the transect, (c): correlation between the surface Sc concentration and the depth of the 17°C isotherm across the transect

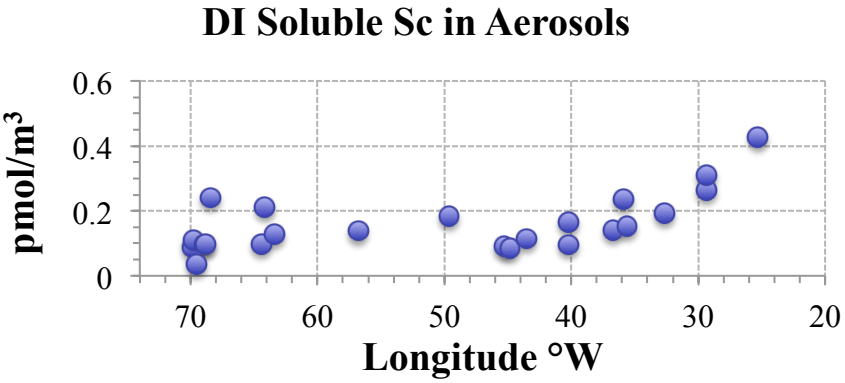

Figure 5: DI soluble Sc in aerosols measured along the North Atlantic transect. Concentration rises on the eastern side of the basin near Africa.

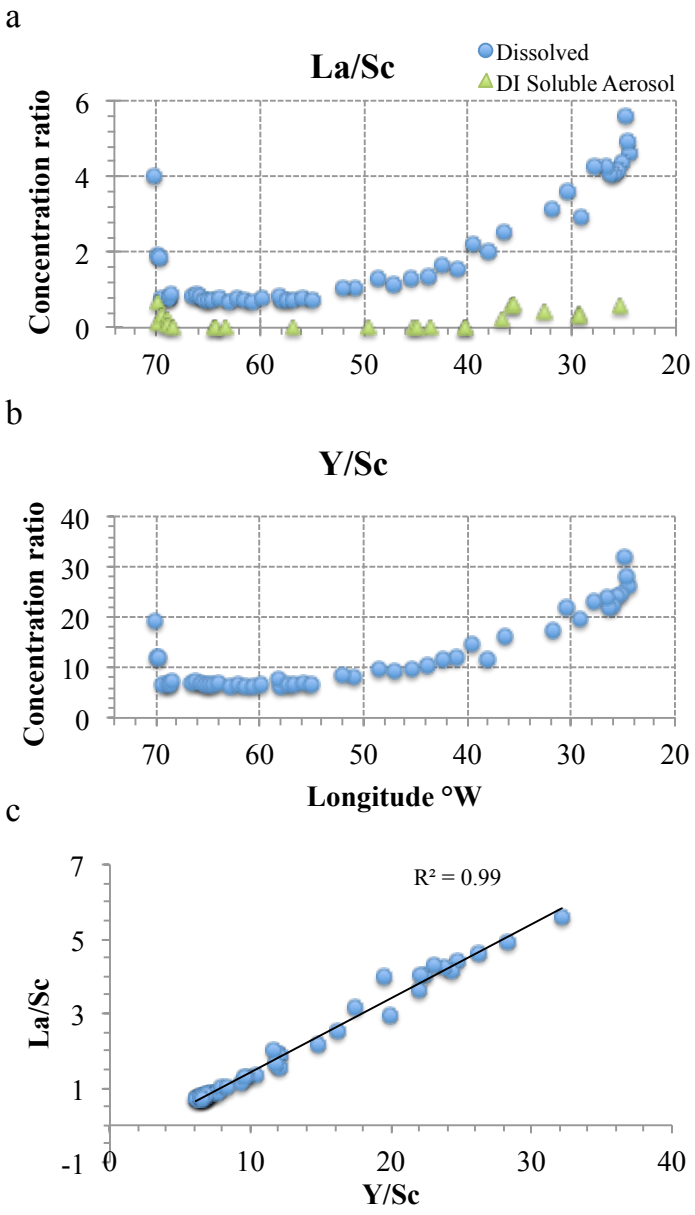

Figure 6 (a): molar ratios of surface dissolved La/Sc (blue circles) and DI soluble aerosol La/Sc (green triangles) along the North Atlantic transect. DI soluble ratios vary minimally across the transect relative to the variation in the dissolved ratio. (b): molar ratios of surface dissolved Y/Sc across the transect. (c): tight correlation between surface dissolved Y/Sc and La/Sc

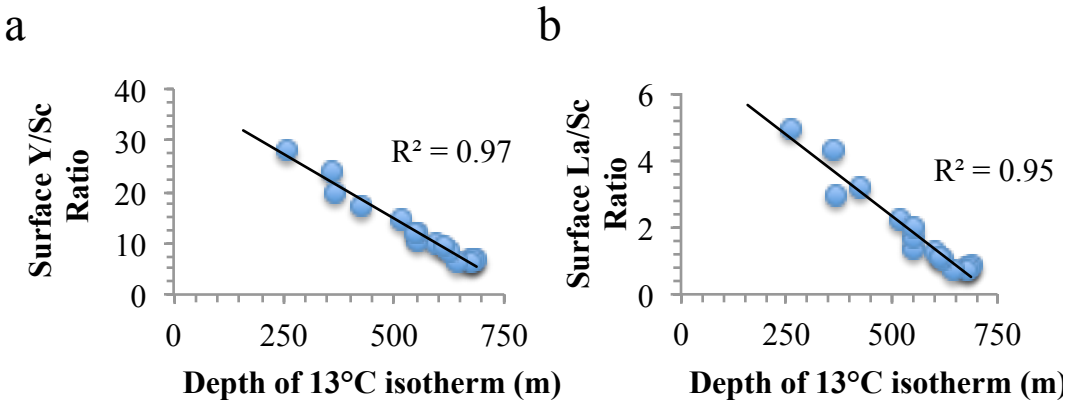

Figure 7: correlations between the depth of the 13°C isotherm and the surface Y/Sc molar ratio (a) and the surface La/Sc molar ratio (b) across the North Atlantic transect.

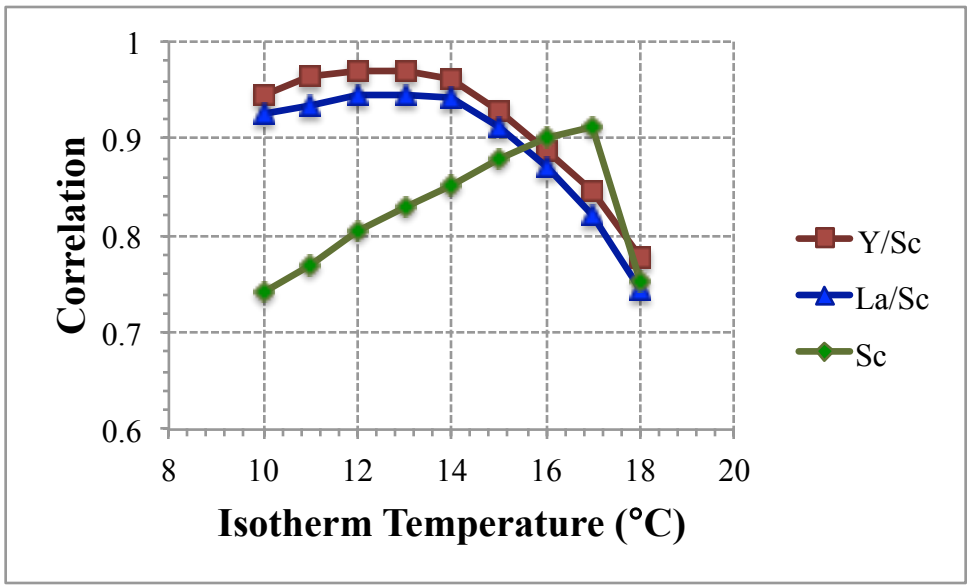

Figure 8: Correlation of analyte with depth of isotherm as a function of selected isotherm temperature. Y/Sc (red squares) and La/Sc (blue triangles) both have a maximum correlation with the depth of the 13°C isotherm, while Sc (green diamonds) has a maximum correlation with the 17°C isotherm. The change in correlation with isotherm temperature is systematic.

CHAPTER 3: IRON LIMITATION OFF THE OREGON COAST

Claire Parker, Tyler Coale, Kenneth Bruland

Abstract

The California Current System is a productive eastern boundary region off the Washington, Oregon, and California coasts. There is strong seasonality to this region, with high levels of rainfall and river input to the coastal ocean during the winter season, and coastal upwelling occurring during the spring and summer. Iron (Fe) input to the coastal ocean during the winter months can be stored in the continental shelf mud belts and then re-suspended and delivered to the surface ocean by upwelling in the spring and summer. There have been many studies providing strong evidence of Fe-limitation of diatom growth occurring in regions of the California Current System off California, and the occurrence of Fe-limitation has been linked with narrow continental shelf mud belt width and low river input. So far, studies off the coasts of Oregon and Washington have shown elevated levels of Fe, due to the wide shelf and high input of Fe from the Columbia River. We present data from July 2014 offshore of the shelf break near Cape Blanco, southern Oregon, a region with moderate shelf width and river input, and find evidence for Fe-limitation of coastal diatom growth rate and biomass accumulation. This observation shows that the Fe-limitation mosaic known to exist off the coast of California extends further north than previously identified, and has implications for models of primary productivity.

1. Introduction

The California Current System is an eastern boundary regime along the Washington, Oregon, and California coasts. Eastern boundary upwelling regimes are characterized by nutrient-rich upwelled water leading to high levels of productivity. For their area, eastern boundary regimes account for a disproportionally large amount of global primary productivity (Carr, 2002), and therefore are important places to study factors governing primary productivity.

There is a strong seasonality to the physical processes occurring in the California Current System that has been well-documented (Huyer, 1983; Lynn and Simpson, 1987; Strub et al., 1987): equatorward, alongshore winds prevail in the spring and summer, which causes the surface waters to move offshore via Ekman transport. Vertical transport compensates for the surface water movement, and high degrees of coastal upwelling ensue: Checkley and Barth (2009) calculated upwelling velocities of 10 to 20 meters per day over the shelf. Upwelled waters are cold, highly saline, and rich in macronutrients, which leads to the high productivity frequently observed in these regions.

Iron, however, it not consistently upwelled in plentiful supply with the macronutrients. Iron is particle reactive and fairly insoluble, leading remineralized Fe to sink out of the water column rather than build up in concentration as the macronutrients do (Bruland et al., 2014). Instead, one of the main Fe sources to eastern boundary regions is the continental shelf (Johnson et al., 1999; Berelson et al., 2003; Bruland et al., 2001; Elrod et al., 2004). Upwelled waters flowing over shelf

sediments can become enriched in Fe, and transport shelf-sourced Fe to the surface along with the other macronutrients (discussed below). This source term of Fe does not vary directly with the upwelling source of macronutrients. As a result, the coastal ocean off of California has been shown to have an Fe-limitation mosaic (Hutchins et al., 1998), with certain regions exhibiting Fe-limitation of diatom blooms (Biller et al., 2013; Bruland et al. 2001; Firme et al., 2003; Hutchins et al., 1998; King and Barbeau, 2007).

Shelf width is an important factor governing the potential for Fe-limitation of phytoplankton growth (Chase et al, 2007; Biller et al., 2013; Hutchins et al., 1998). While the upwelling conditions are in the spring and summer, winter rains and storms lead to high river runoff delivering Fe to the coastal ocean. Much of the riverine suspended sediment input to the ocean sinks onto the continental shelf mud belts at depths of 50-90 m (Wheatcroft et al., 1997; Xu et al., 2002), but Fe-rich particles can be re-suspended from the shelf and upwelled to the surface during the spring/summer upwelling season (Johnson et al., 1999). In regions where there is a wide shelf in the 50-90 m depth range, there is more area to retain the Fe-rich riverine sediment, and more contact between the upwelling water and the mud belt sediment, leading to greater Fe supplied from coastal upwelling. Furthermore, reduced dissolved Fe in the shelf sediment can flux into the water column and be upwelled from the shelf to the surface ocean as well, which comprises another significant source of Fe (Berelson et al., 2003; Elrod et al., 2004). As a result of these processes, in the California Current

System both river input and shelf width are linked to phytoplankton biomass (Chase et al., 2007).

Previous studies identifying Fe-limitation in the California Current System have focused on regions off the coast of California (Biller et al., 2013; Bruland et al. 2001; Firme et al., 2003; Hutchins et al., 1998; King and Barbeau, 2007). On the other hand, Lohan and Bruland (2008) investigated Fe inputs off the coast of northern Oregon and Washington and found elevated concentrations of Fe due to the broad shelf and high riverine input from the Columbia River. In this work we present data from a region of the California Current System off the coast of southern Oregon near Cape Blanco, offshore of a moderately narrow shelf, where we sampled in July 2014. We provide evidence for Fe-limitation of coastal diatoms in this region as well.

2. Methods

2.1 Study Site and Sample Collection

The IRNBRU cruise took place off the coasts of California and Oregon in July 2014 aboard the R/V Melville. We report surface temperature and salinity along with dissolved Fe, nitrate, phosphate, silicic acid, and chlorophyll *a* concentration data from two transects off the coast of Oregon near Cape Blanco, which we sampled on July 20th, 2014. Figure 1 shows sampling locations overlaid on sea surface temperature (Figure 1a) and mean sea level anomaly (Figure 1b) for that day. Throughout the cruise, we monitored satellite data of surface altimetry and sea surface temperature daily, and adjusted the cruise plan in order to best capture the

current features. We targeted our investigations to upwelling and potentially Fe-limited regions. Surface hydrographic data (temperature, salinity, and fluorescence) were monitored with the ship's flow-through underway data system. Chlorophyll *a* concentrations were derived from fluorescence data from the flow-through fluorometer, which was calibrated to chlorophyll *a* using the method of Welschmeyer (1994). Nutrient samples were analyzed for nitrate+nitrite, phosphate, and silicic acid with a Lachat QuickChem 800 Flow Injection Analysis System and standard spectrophotometric methods (Parsons et al., 1984). Surface samples as well as vertical profile samples were taken and analyzed for dissolved Fe shipboard with a method adapted from Lohan et al. (2006) (discussed below).

Surface samples were obtained through a surface tow-fish system (Bruland et al., 2005). The fish swam in the surface water alongside the ship, deployed from the end of a boom off the starboard side. Seawater was cleanly pumped through Teflon lines throughout the ship. Nutrient analyses were performed every 1.5 minutes on the water flowing out the terminus of the Teflon line. Surface Fe samples were obtained from a valve earlier in this line. Iron samples were filtered through a 0.2 μm polysulfone membrane AcroPak-200® capsule filter into low-density polyethylene bottles that had been rigorously cleaned as in the GEOTRACES cookbook (Cutter et al., 2014). Sample bottles for Fe were stored in weak (pH ~2) trace metal grade HCl and rinsed three times with sample before filling. Iron samples were acidified to pH ~2 with the equivalent of 2 mL of 6 N quartz-distilled HCl and let sit for at least an hour before analysis.

2.2 Shipboard Fe analysis method

Iron analysis was performed shipboard to give us near-real-time data, allowing us to better plan the rest of the cruise. The method used for this is based on Lohan et al. (2006), and involves preconcentrating the dissolved Fe on a chelating resin before adding the colorimetric agent N,N- dimethyl-p-phenylenediamine dihydrochloride (DPD), and detecting the catalytically enhanced signal with a UV-vis spectrophotometer. The seawater is loaded onto the resin at pH 2 because the Fe(III) that had been chelated with organic compounds is dissociated at pH 2 and available to chelate with the resin. Additionally, loading at a low pH is advantageous when working with high concentrations of Fe that are insoluble at higher pHs. Lohan et al. (2006) used the NTA-type superflow resin, but due to lower blanks and better consistency, we followed the change by Biller et al. (2013) and used Toyopearl Chelate-650 instead. Since Fe(II) is not recovered at pH 2 on this resin, whereas Fe(III) is recovered at >93% (Biller et al., 2013), 10 μmol/L H_2O_2 is added to the sample before loading, which is sufficient to quantitatively oxidize any reduced Fe present in the sample (Lohan et al., 2005).

2.3 Satellite data

Temperature data from the NOAA POES AVHRR satellite was downloaded from the NOAA coastwatch website (http://coastwatch.pfeg.noaa.gov/coastwatch/CWBrowser.jsp?), and altimetry data was produced (including merging data from multiple satellites) and distributed by Aviso (http://www.aviso.altimetry.fr/). The availability of temperature data was

inconsistent due to frequent interference by clouds, but altimetry data was reliably available daily. We imaged the satellite data with Interactive Data Language®, a product of Exelis Visual Information Solutions, Inc., a subsidiary of Harris Corporation (Exelis VIS).

3. Results and Discussion

3.1 Overview of transects

The summer of 2014 was a summer with unusually low wind and coastal upwelling in the California Current System (Zaba and Rudnick, 2016). Along the California coastline, significantly less upwelling occurred in summer 2014 than usual, and the southern Oregon coastline was the furthest south region of the California Current System exhibiting active upwelling during our research cruise. Figure 1 shows the two transects that we sampled off the southern Oregon coast. Transect 9 (the east/west transect) immediately followed completion of transect 8 (the north/south transect). The ~10°C water in Figure 1a shows the active upwelling occurring at the time we sampled, and the geostrophic flow of the anticyclonic and cyclonic eddies in Figure 1b (labeled 1 and 2, respectively) is moving that plume of upwelled water between the two eddies: offshore and to the southwest.

Figure 2 shows the temperature, salinity, chlorophyll *a*, nitrate, and dissolved Fe along transect 8. On the northern end of the transect, there is clear evidence of upwelling with the low temperatures (~9.9-10.6°C) and high salinities (33.3-33.7). The lowest temperature and highest salinity occur at about 42.3°N, and there is a

corresponding increase in the nitrate and silicic acid concentrations at this latitude. Despite the active upwelling inferred from the low temperature and high salinity values, and the resulting high concentrations of nitrate, phosphate, and silicic acid (21 μmol/kg, 1.6 μmol/kg, and 24 μmol/kg, respectively), the chlorophyll *a* is relatively low (2.5-3.3 μg/L). Dissolved Fe has a maximum concentration of 0.7 nmol/kg, which occurs at 42.4°N; at this same location there is a slight decrease in the nitrate and silicic acid concentrations and a slight increase in the temperature, but the salinity is still high at that location. This could be indicative of a plume of slightly older upwelled water that has had time to warm and have the nutrients be slightly drawn down.

Transect 9 exhibits similar characteristics to transect 8 (Figure 3). There are low temperatures (10.1-10.6 °C) and high salinities (33.4-33.7) in the eastern part of the transect, corresponding with high nitrate (17-21 μmol/kg), phosphate (1.3-1.6 μmol/kg) and silicic acid (18-23 μmol/kg), indicative of upwelling. Meanwhile the chlorophyll *a* remains relatively low (1.1-3.8 μg/L), as does the dissolved Fe concentration (0.35-0.4 nmol/kg), in the upwelling zone. At 125.3° W, the salinity and nutrients dropped markedly as the transect moved out of the upwelled water and into low salinity water influenced by the California Current. As a result, we changed directions and headed southwest back into the high salinity and nutrient rich upwelled waters. At the western end of the transect there was a marked salinity drop and rise in temperature as the transect left the upwelling filament and began to enter the anticyclonic eddy (labeled "1" on Figure 1b).

After upwelling, nutrient concentrations can decrease both by being drawn down through assimilation by phytoplankton and by dilution as the highly saline, nutrient-rich upwelled water mixes with the low salinity, low-nutrient California Current surface water. Plots of nutrients versus salinity should clarify which of these factors is dominant in impacting the nutrient concentrations. Due to the range of upwelling signature across the two transects, we divide the region into zones. Figure 4 shows the surface salinity across both transects. The strongest upwelling signal is a plume identifiable by its high salinity (zone 1), and we crossed that plume twice. We define the boarders of the upwelling zone to be when salinity transitions to 33.4, both times we crossed the upwelling plume. That leaves a region north of the plume with lower salinity (zone 2), the western part of transect 9 (zone 3), and the southern part of transect 8 (zone 4).

Measured attributes (temperature, nitrate, phosphate, silicic acid, chlorophyll *a*, and dissolved Fe) plotted against salinity for each of these zones are shown in Figure 5. In general, temperature is indirectly related to salinity, and the macronutrients nitrate, phosphate, and silicic acid are directly related to salinity. These trends are expected based on upwelling of low temperature, high salinity, nutrient-rich waters, and mixing with the California Current surface water. There is some evidence of macronutrient drawdown in western transect 9 and southern transect 8, with macronutrient concentrations lower for a given salinity than they would be from a mixing line. The western region of transect 9 and the southern region of transect 8 are remarkably similar in salinity space, with the exception of

chlorophyll *a*, which is higher along transect 9. The relatively high chlorophyll *a* concentrations in western transect 9 fits with nutrient draw down, while southern transect 8 could have had a bloom previously. The northern peak exhibits the most distinct characteristics of all the zones, with higher macronutrient concentrations and lower temperatures than the other parts of the study site, and yet does not have correspondingly higher chlorophyll *a*. Chlorophyll *a* shows no trend with salinity, nor does Fe except at the highest salinity values indicating there is some source of Fe from upwelling in this region.

3.2 Investigation of Fe-limitation of diatoms

The low Fe concentrations, high macronutrient concentrations, and relatively low chlorophyll *a* in the upwelling regions of these transects indicate that Fe-limitation is likely. Biller et al. (2013) utilized two methods for investigating the extent of Fe limitation in the California Current System by approaching the limitation from the perspectives of growth rate and biomass accumulation. We choose to follow the lead of Biller et al. (2013), and for both methods compare Fe and nitrate as potential limiting nutrients.

Growth rates for specific types of phytoplankton can be calculated based on nutrient availability and half saturation constants with the following well-established equation (Monod, 1942):

$$\mu = \mu_{max}[S]/([S] + K_{\mu})$$

where μ is the growth specific growth rate (under the conditions specified), μ_{max} is the maximum growth rate under optimal conditions, [S] is the ambient concentration of

the nutrient, and K_μ is the half-saturation constant for the nutrient (where $\mu=0.5\mu_{max}$). Sarthou et al. (2005) compiled and reported values of μ_{max} and K_μ for diatoms. As in Biller et al. (2013), we choose to estimate diatom growth rate using the average values reported by Sarthou et al. (2005): μ_{max} = 1.5 d^{-1}, K_μ for Fe = 0.35 nmol L^{-1}, K_μ for N = 1.6 μmol L^{-1}. In a given time and place, the nutrient with the smallest specific growth rate is considered the growth-rate limiting nutrient. Since we have chosen to compare Fe and nitrate as potential limiting nutrients, where the specific growth rate calculated based on Fe concentrations (μ_{Fe}) is less than that based on the nitrate concentrations (μ_{NO3-}) there is evidence that Fe is the growth-rate limiting nutrient.

Calculated growth rates based on the Fe and nitrate concentrations along the two transects are depicted in Figure 6. Again, any locations where the μ_{Fe} is lower than the μ_{NO3-} indicate evidence of Fe limitation of coastal diatoms. There is one region in transect 9 (~125.3°W) where the nitrate concentrations are less than 2 μmol/kg and the μ_{NO3-} is less than the μ_{Fe}. Besides that location, the entirety of both transects show evidence of low Fe concentrations limiting the growth rate of coastal diatoms as well as their ability to accumulate biomass.

The other way that Biller et al. (2013) used to estimate Fe-limitation is by considering biomass accumulation. Coastal diatoms grow at near-optimal rates at 30 μmol/mol Fe to carbon (Sunda and Huntsman, 1995; Bruland et al. 1991). Using the Redfield ratio for carbon to nitrogen (Redfield, 1958), Biller et al. (2013) calculate a required Fe to nitrate ratio of 0.2 nmol/μmol. Therefore if the ambient Fe to nitrate

ratio is less than 0.2 nmol/μmol, coastal diatoms would be limited in their biomass accumulation by Fe rather than by nitrate. Biller et al. (2013) extended the calculation to oceanic diatoms with a Fe to carbon ratio of 10 μmol/mol (Sunda and Huntsman, 1995) and calculate that the biomass accumulation of oceanic diatoms would be Fe-limited at Fe to nitrate ratios of 0.07 nmol/μmol and below. An advantage to this method of investigating Fe-limitation is that there is no concern about the delay between upwelling and phytoplankton growth: where Fe to nitrate ratios are less than 0.2 nmol/μmol, we can say that even if a bloom were to happen, Fe would limit the biomass accumulation of coastal diatoms.

The Fe to nitrate ratio for both transects is depicted in Figure 7 for all locations where both Fe and nitrate were measured and nitrate was greater than 4 μmol/kg. All samples are below 0.2 nmol/μmol Fe to nitrate, indicating that Fe is the Liebig limiting nutrient for coastal diatoms. Furthermore, all samples on transect 8 and most along transect 9 are below 0.07 nmol/μmol Fe to nitrate, indicating that oceanic diatoms as well would be limited in biomass accumulation by Fe in this region.

Evidence of Fe-limitation from both Liebig limitation and growth rate calculations is a strong indication of Fe-limitation of coastal diatoms in this region. This is the furthest north region of the California Current System that has been found to have evidence of Fe-limitation, which extends the known range of the Fe-limitation mosaic, and could be useful to include in global models of primary productivity.

Since Fe-limitation in the California Current System has been often connected with narrow shelf width (Biller et al., 2013; Chase et al. 2007; Hutchins et al. 1998), it is at first surprising that the region in which we observe evidence of Fe-limitation has a moderate shelf (Figure 8). When Lohan and Bruland (2008) found elevated Fe in the shelf waters off the northern coast of Oregon, they sampled at a wide-shelf region inland of the shelf break and close to the Columbia River mouth (Figure 8), which is a large source of Fe to the shelf in that region (Bruland et al., 2008). However, we were much further away from the Columbia River, and we sampled offshore of the shelf break (Figure 8). Kudela et al. (2006) have identified an "iron curtain" effect with rapidly decreasing Fe concentrations off the continental shelf off the coast of California, which has also been observed in the Peru upwelling system (Bruland et al., 2005). It is possible that a similar decrease in the surface Fe concentration occurs off this shelf break along the Oregon coastline. Since there is a moderate shelf width and river input off the southern coast of Oregon, it is possible that over the shelf there is sufficient supply of Fe.

4. Conclusions

We find evidence of Fe-limitation of coastal diatoms off the southern Oregon coast. Two methods of evaluating Fe-limitation were used to investigate this possibility: Fe to nitrate ratios to determine the Liebig limiting nutrient on biomass accumulation, and calculation of growth rates based on the ambient nitrate and Fe concentrations. Both methods indicate that coastal diatoms are limited by Fe in most locations of the two transects we analyzed. In comparison with previous work off the

northern coast of Oregon that showed elevated Fe (Lohan and Bruland, 2008), this work is further from the Columbia River mouth, and offshore of the shelf break rather than over the shelf. Identifying evidence of Fe-limitation off the southern Oregon coast, further north than any previously documented Fe-limitation in the California Current System, indicates that this Fe-limitation mosaic is a more widely spread phenomena than previously known and has implications for models of global primary productivity.

Acknowledgements

The authors thank the captain and crew of the R/V Melville, Dondra Biller for her vast assistance with flow injection analysis, satellite imaging code, and for downloading satellite data while we were at sea, and Geoffrey Smith, Travis Mellett, and Matthew Brown for assistance with sample collection. This work was funded by the National Science Foundation through award number OCE 1259776.

References

Berelson, W., J. McManus, K. Coale, K. Johnson, D. Burdige, T. Kilgore, D. Colodner, F. Chavez, R. Kudela, and J. Boucher (2003), A time series of benthic flux measurements from Monterey Bay, CA, Cont. Shelf Res., 23, 457–481, doi:10.1016/S0278-4343(03)00009-8.

Biller, D.V., T.H. Coale, R.C. Till, G.J. Smith, and K.W. Bruland (2013), Coastal iron and nitrate distributions during the spring and summer upwelling season in the central California Current upwelling regime, Cont. Shelf Res., 66, 58-72, doi: 10.1016/j.csr.2013.07.003.

Bruland, K.W., E.L. Rue, and G.J. Smith (2001), Iron and macronutrients in California coastal upwelling regimes: implications for diatom blooms, Limnol. Oceanogr., 46, 1661–1674, doi: 10.4319/lo.2001.46.7.1661.

Bruland, K.W., E.L. Rue, G.J. Smith, and G.R. Ditullio (2005), Iron, macronutrients and diatom blooms in the Peru upwelling regime: brown and blue waters of Peru, Mar. Chem., 93, 81–103, doi:10.1016/j.marchem.2004.06.011.

Bruland, K.W., M.C. Lohan, A.M. Aguilar-Islas, G.J. Smith, B. Sohst, and A. Baptista (2008), Factors influencing the chemistry of the near-field Columbia River plume: Nitrate, silicic acid, dissolved Fe, and dissolved Mn, J. Geophys. Res., C00B02, doi:10.1029/2007JC004702.

Bruland, K.W., R. Middag, and M.C. Lohan (2014), Controls of trace metals in seawater, Treatise on Geochemistry (2nd edition), Elsevier, Oxford, [ISBN: ISBN: 978-0-08-098300-4],19-51, doi:10.1016/B978-0-08-095975-7.00602-1.

Carr, M.E., (2002), Estimation of potential productivity in Eastern Boundary Currents using remote sensing, Deep-Sea Res. Pt. II, 49, 59–80, doi: 10.1016/S0967-0645(01)00094-7.

Chase, Z., P.G. Strutton, and B. Hales (2007) Iron links river runoff and shelf width to phytoplankton biomass along the US West Coast, Geophys. Res. Lett., 34, LO4607, doi: 10.1029/2006GL028069.

Checkley, D.M., and J.A. Barth (2009), Patterns and processes in the California Current System, Prog. Oceanogr., 83, 49–64, doi: 10.1016/j.pocean.2009.07.028.

Cutter, G. A., P. Andersson, L. Codispoti, P. Croot, R. Francois, M. Lohan, H. Obata, and M. R. van der Loeff (2014), Sampling and sample-handling protocols for GEOTRACES cruises, version 2.0,

http://www.geotraces.org/images/stories/documents/intercalibration/Cookbook.pdf

Elrod, V.A., W.M. Berelson, K.H. Coale, and K.S. Johnson (2004), The flux of iron from continental shelf sediments: a missing source for global budgets, Geophys. Res. Lett., 31, L12307, doi:10.1029/2004GL020216.

Firme, G.F., E.L. Rue, D.A. Weeks, K.W. Bruland, and D.A. Hutchins (2003), Spatial and temporal variability in phytoplankton iron limitation along the California coast and consequences for Si, N, and C biogeochemistry, Global Biogeochem. Cycles, 17, 1016, doi:10.1029/2001GB001824.

Hutchins, D.A., G.R. Ditullio, Y. Zhang, and K.W. Bruland (1998), An iron limitation mosaic in the California upwelling regime, Limnol. Oceanogr., 43, 1037–1054, doi: 10.4319/lo.1998.43.6.1037.

Huyer, A. (1983), Coastal upwelling in the California Current System, Prog. Oceanogr., 12, 259–284, doi:10.1016/0079-6611(83)90010-1.

Johnson, K.S., F.P. Chavez, and G.E. Friederich (1999), Continental-shelf sediment as a primary source of iron for coastal phytoplankton, Nature, 398, 697–700, doi: 10.1038/19511.

King, A.L., and K. Barbeau (2007), Evidence for phytoplankton iron limitation in the southern California Current System, Mar. Ecol.-Prog. Ser., 342, 91–103, doi: 10.3354/meps342091.

Kudela, R., N. Garfield, and K. Bruland (2006), Bio-optical signatures and biogeochemistry from intense upwelling and relaxation in coastal California, Deep-Sea Res. Pt. II., 53, 2999-3022.

Lohan, M.C., and K.W. Bruland (2008), Elevated Fe(II) and dissolved Fe in hypoxic shelf waters off Oregon and Washington: and enhanced source of iron to coastal upwelling regimes, Environ. Sci. Technol., 42, 6462–6468, doi: 10.1021/es800144j.

Lohan, M.C., A.M. Aguilar-Islas, R.P. Franks, and K.W. Bruland (2005), Determination of iron and copper in seawater at pH 1.7 with a new commercially available chelating resin, NTA Superflow, Anal. Chim. Acta., 530, 121-129, doi:10.1016/j.aca.2004.09.005.

Lohan, M.C., A.M. Aguilar-Islas, and K.W. Bruland (2006), Direct determination of iron in acidified (pH 1.7) seawater samples by flow injection analysis with

catalytic spectrophotometric detection: application and intercomparison. Limnol. Oceanogr.-Meth., 4, 164–171, doi: 10.4319/lom.2006.4.164.

Lynn, R.J., and J. J. Simpson (1987), The California Current System: the seasonal variability of its physical characteristics, J. Geophys. Res., 92(C12), 12947–12966, doi:10.1029/JC092iC12p12947.

Parsons, T.R., Y. Maita, and C.M. Lalli (1984), A Manual of Chemical and Biological Methods for Seawater Analysis, Pergamon Press Ltd., Great Britian.

Redfield, A.C., (1958), The biological control of chemical factors in the environment, American Scientist, 46, 205–221.

Sarthou, G., K.R. Timmermans, S. Blain, and P. Treguer (2005), Growth physiology and fate of diatoms in the ocean: a review, J. Sea Res., 53, 25–42, doi:10.1016/j.seares.2004.01.007.

Strub, P.T., J.S. Allen, A. Huyer, and R.L. Smith (1987), Large-scale structure of the spring transition in the coastal ocean off western North America, J. Geophys. Res., 92(C2), 1527–1544, doi:10.1029/JC092iC02p01527.

Sunda, W.G., and S.A. Huntsman (1995), Iron uptake and growth limitation in oceanic and coastal phytoplankton, Mar. Chem., 50, 189–206, doi: 10.1016/0304-4203(95)00035-P.

Welschmeyer, N.A. (1994), Fluorometric analysis of chlorophyll a in the presence of chlorophyll b and Pheopigments, Limnol. Oceanogr., 39, 1985–1992, doi:10.4319/lo.1994.39.8.1985.

Wheatcroft, R.A., C.K. Sommerfield, D.E. Drake, J.C. Borgeld, and C.A. Nittrouer (1997), Rapid and widespread dispersal of flood sediment on the northern California margin, Geology, 25(2), 163–166, doi:10.1130/0091-7613(1997)025<0163:RAWDOF>2.3.CO;2.

Xu, J.P., M. Noble, and S.L. Eittreim (2002), Suspended sediment transport on the continental shelf near Davenport, California, Mar. Geol., 181, 171–193, doi: 10.1016/S0025-3227(01)00266-3.

Zaba, K.D., and D.L. Rudnick (2016), The 2014-2015 warming anomaly in the Southern California Current System observed by underwater gliders, Geophys. Res. Lett., 43, doi:10.1002/2015GL067550.

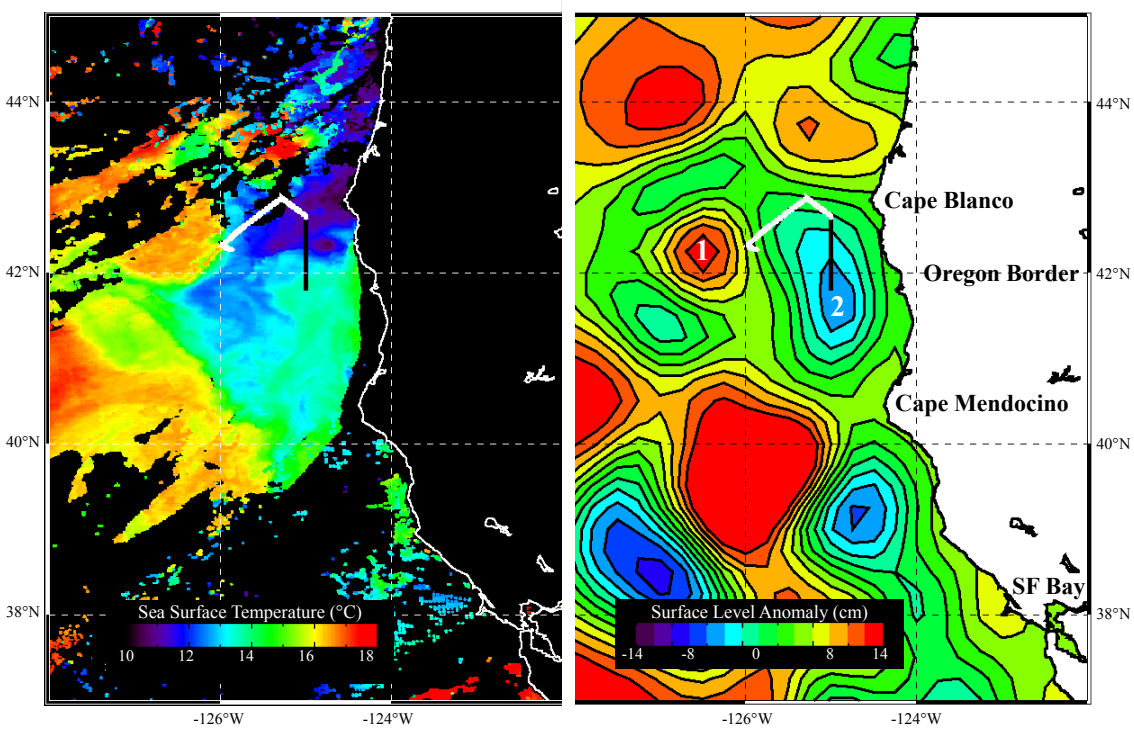

Figure 1: Sea surface temperature and mean surface level anomaly on July 20th, 2014, off the Oregon and Northern California coasts with the two transects we completed that day overlaid (transect 8, in black, and transect 9, in white). The anticyclonic and cyclonic eddies that are contributing to the movement of the upwelled plume of water offshore are labeled 1 and 2, respectively.

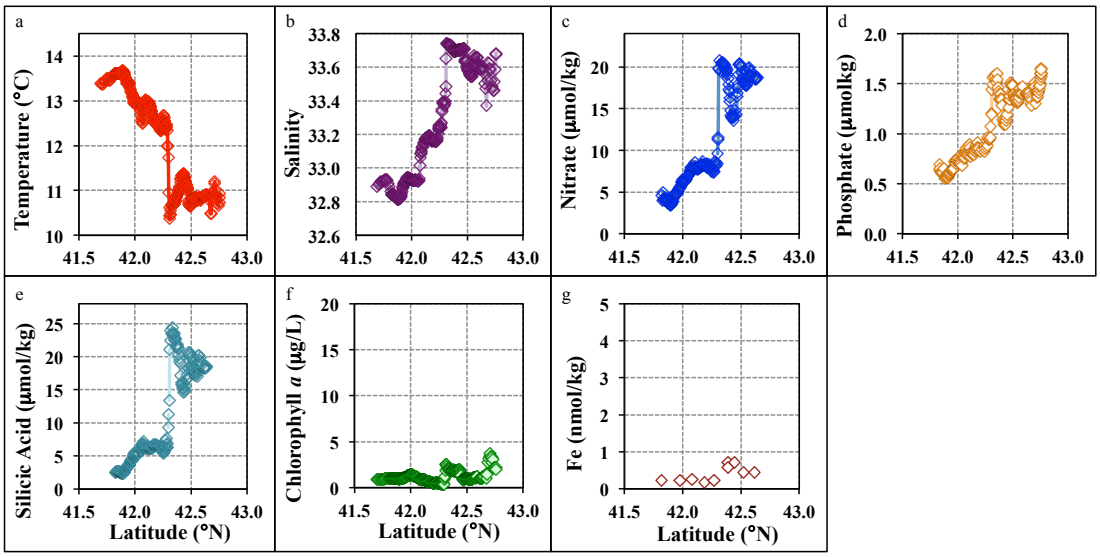

Figure 2: Temperature (a), salinity (b), nitrate (c), phosphate (d), silicic acid (e), chlorophyll *a* (f) and dissolved Fe (g) versus latitude along transect 8.

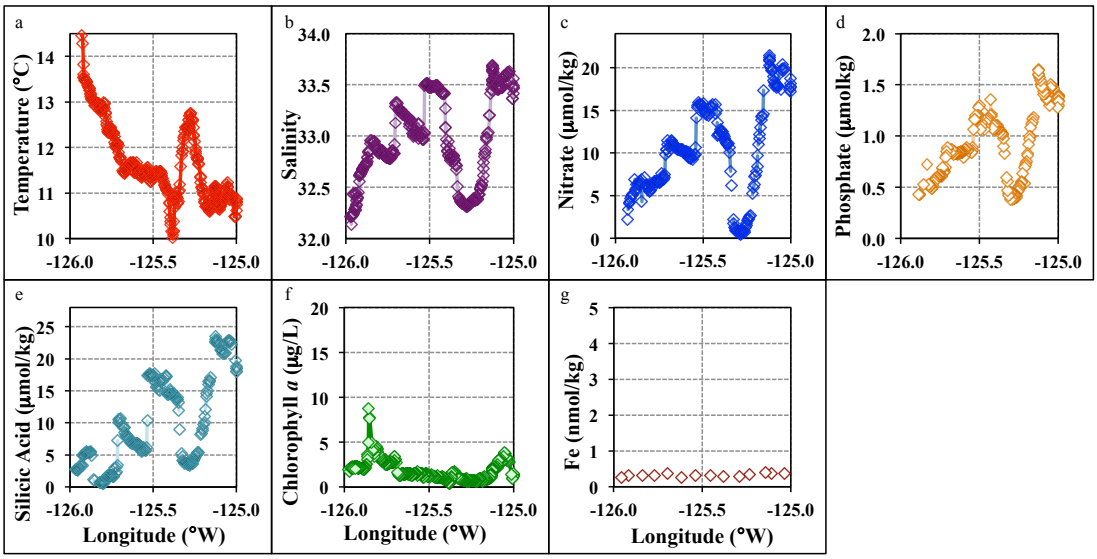

Figure 3: Temperature (a), salinity (b), nitrate (c), phosphate (d), silicic acid (e), chlorophyll *a* (f) and dissolved Fe (g) versus longitude along transect 9.

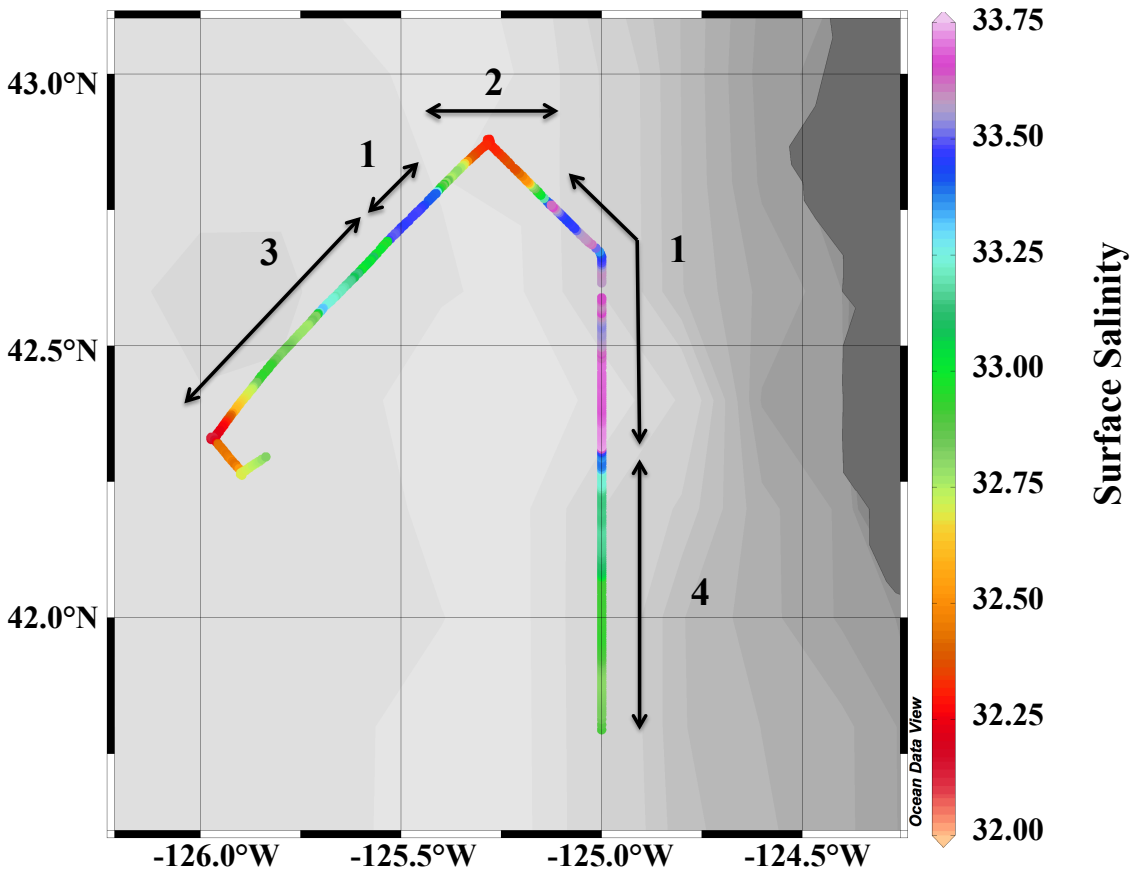

Figure 4: Surface salinity along both transects. Note that cooler colors (purple, blue) correspond with higher salinities. The upwelling plume (zone 1), identifiable by its high salinity, was crossed twice. North of the upwelling plume there is a decrease in salinity (zone 2). The remaining western part of transect 9 and southern part of transect 8 are zones 3 and 4, respectively.

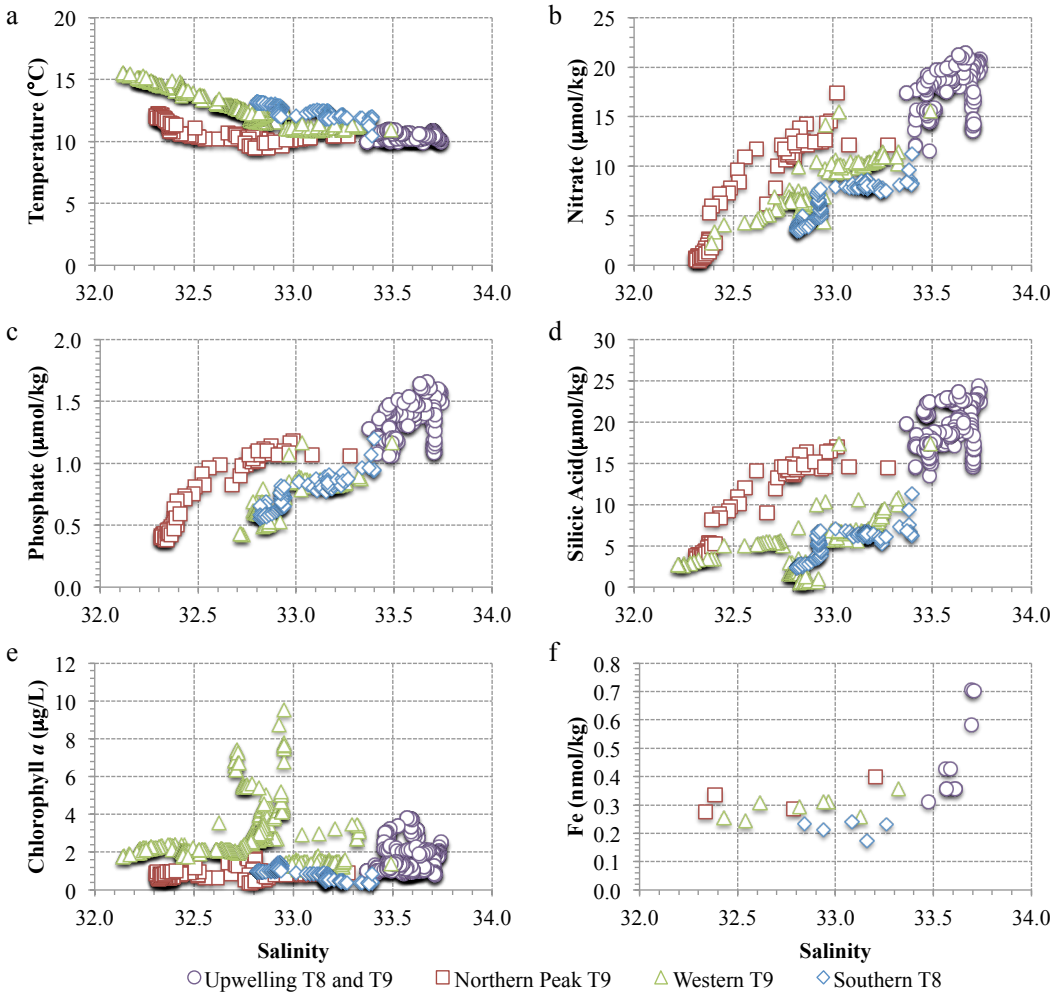

Figure 5: Temperature (a), nitrate (b), phosphate (c), silicic acid (d), chlorophyll *a* (e) and dissolved Fe (f) versus salinity for both transect 8 and transect 9. The transects are split into zones based on salinity transitions across 33.4: Southern T8: transect 8 south of the major salinity transition at 33.4; Upwelling T8 and T9: the upwelling region that we crossed twice defined by major salinity transitions at 33.4; Western T9: transect 9 west of the major salinity transition at 33.4; Northern Peak T9: the northern most part of T9, north of the upwelling zone.

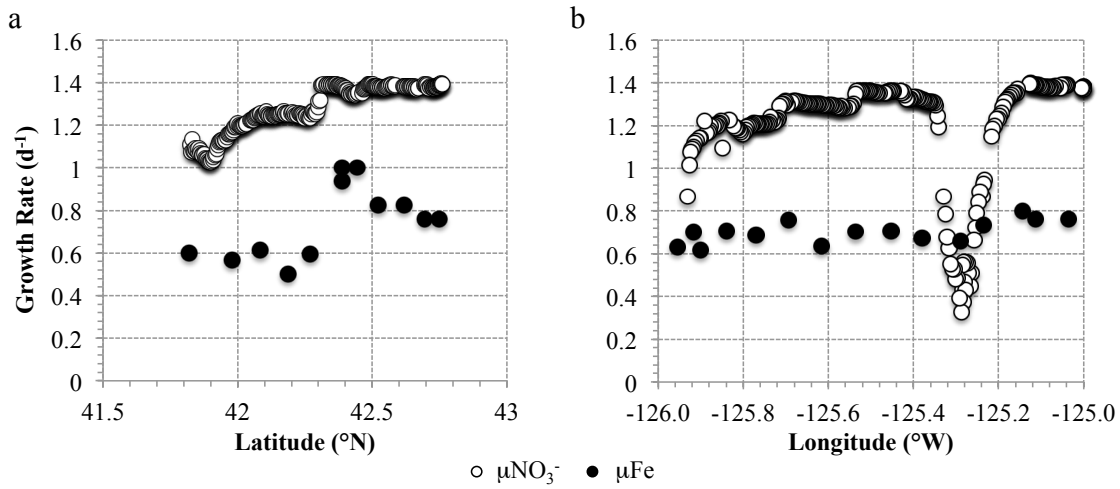

Figure 6: Estimated growth rate calculated from Fe (μ_{Fe}) and nitrate (μ_{NO3-}) concentrations on transect 8 (a) and transect 9 (b). A μ_{Fe} lower than the μ_{NO3-} suggests that Fe is limiting diatom growth rate in that location.

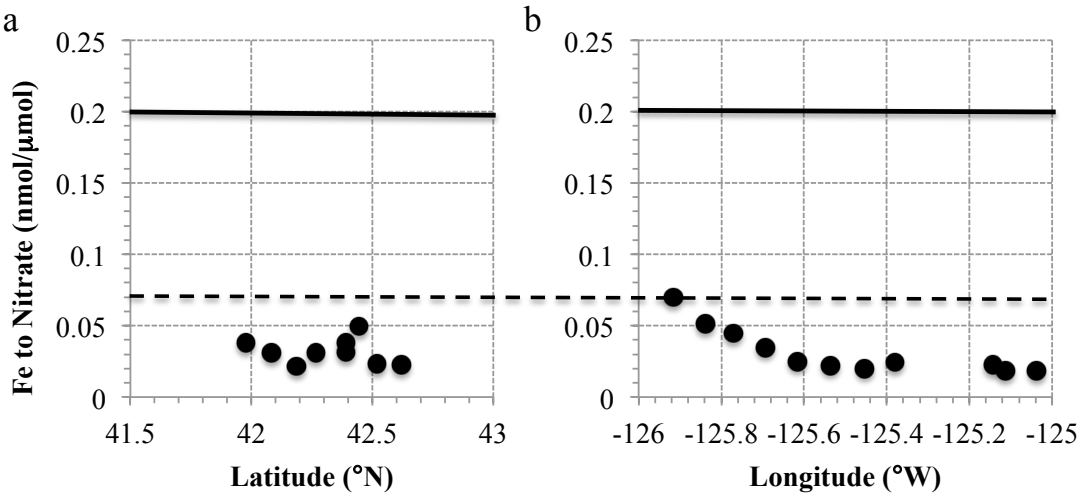

Figure 7: Iron to nitrate ratio for transect 8 (a) and transect 9 (b) where nitrate concentrations are greater than 3.5µmol/kg. Note the different measurements on the x-axes. A ratio below 0.2 nmol/µmol (solid black line) suggests Liebig limitation of coastal diatoms, and a ratio below 0.07 nmol/µmol (dotted black line) suggests the same for oceanic diatoms.

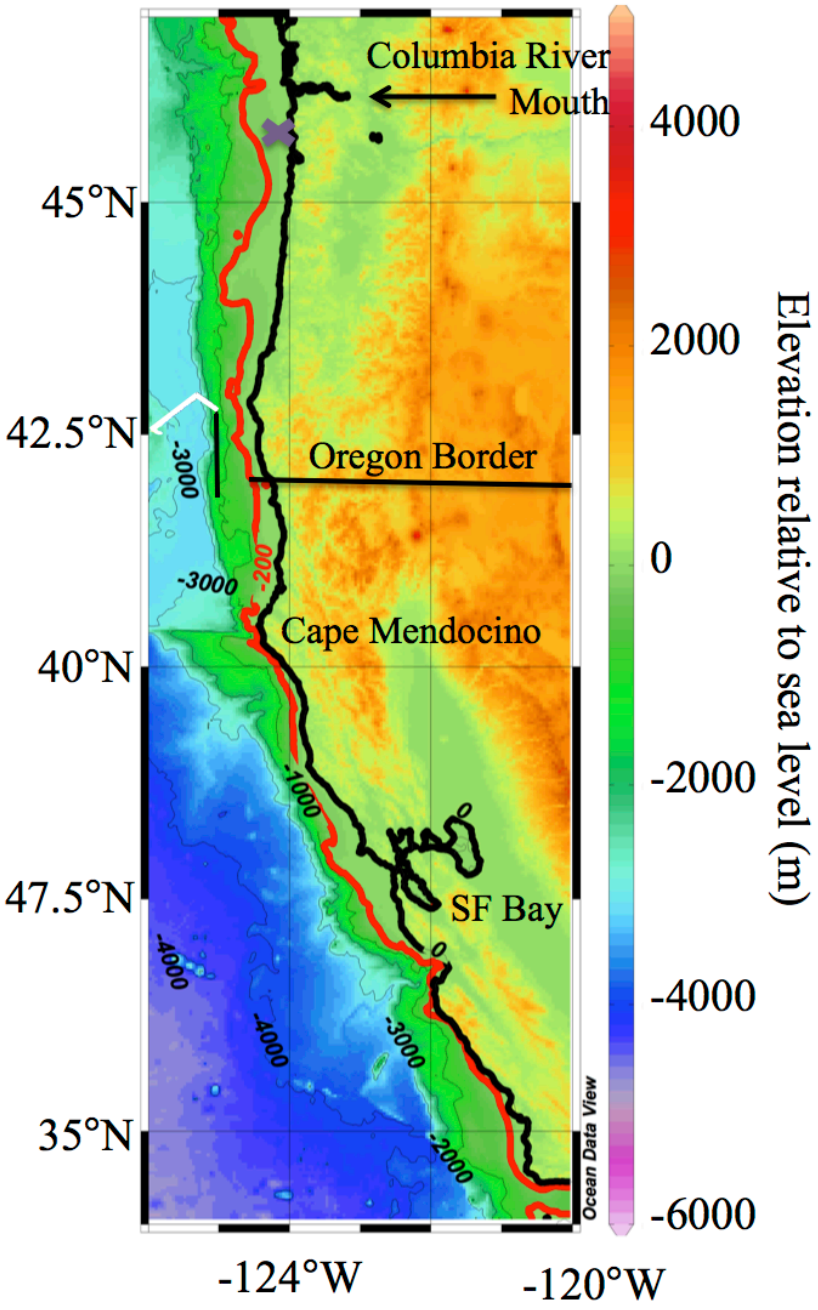

Figure 8: Shelf width along the northern California and Oregon coastline. The red line marks the 200 m isobath. The cruise tracks for this work are overlaid in black (transect 8) and white (transect 9). Lohan and Bruland [2008]'s Oregon shelf sampling location is marked by the purple cross.

CONCLUSION

The first part of this dissertation greatly expands on the knowledge base of dissolved Sc in the ocean, and presents two promising applications of the newfound knowledge: the potential that Sc distributions reflect the non-nutrient side of the Fe distribution, and the possibility to use surface Sc removal as an indicator of scavenging intensity or export production. The latter part extends our understanding of the Fe-limitation mosaic of the California Current System further north, with evidence for Fe-limitation of coastal diatoms near Cape Blanco, off the southern coast of Oregon.

In Chapter 1, we published the first modern multi-basin dataset of dissolved Sc in the ocean. We were able to conclude from the nutrient-like shape of the depth profiles and similar concentrations in the deep-water of the North Atlantic and North Pacific that Sc is a hybrid-type metal as defined by Bruland and Lohan (2003) and Bruland et al. (2014), with its distribution governed significantly by both remineralization and scavenging. Based on a comparison between the deep-water North Atlantic to North Pacific concentration ratios between Sc and other well-characterized metals, we inferred an oceanic residence time of Sc of about 1000 years.

We also examine the similarity between Sc and Fe in distribution and reactivity. Both have an inorganic speciation of Metal-$(OH)_3^0$ (Byrne, 2002), which suggests that Fe and Sc might have similar reactivity. Indeed, Rogers et al. (1980) found evidence for Sc substituting for Fe in Fe-binding organic complexes, and in

Chapter 1 we observe that the deep-water North Atlantic to North Pacific concentration ratios of Fe and Sc are very similar. Despite all these similarities between the metals, Fe is an essential micronutrient while Sc is not known to have any biological use. Chapter 1 proposes that the distribution of dissolved Sc may be representative of the non-nutrient side of the oceanic Fe distribution, and could be useful in teasing apart the many facets of oceanic Fe cycling.

In Chapter 2, we investigate the possibility of using Sc removal by scavenging in the surface ocean as an indicator of scavenging intensity, potentially specifically of scavenging by export production. We demonstrate that the Y/Sc and La/Sc ratios input to the surface North Atlantic are relatively constant compared to the Y/Sc and La/Sc ratios in the dissolved surface ocean. Since Sc is more particle reactive than Y and La (Parker et al., accepted), we assume that the surface dissolved ratios deviate from the input ratios as a result of Sc removal by scavenging. We demonstrate that the surface Y/Sc and La/Sc ratios are highly correlated with the depth of the 13°C isotherm (R^2=0.97 and 0.95, respectively, simple linear regression), and therefore the shape of the gyre. Surface export production generally follows this same pattern. We propose that at the boundaries of the gyre, where the nutriclines are closer to the surface, there is increased delivery of nutrients to the surface, increased export production, and increased Sc removal, and that therefore surface Sc removal as observed by surface Y/Sc and La/Sc ratios could be an indicator of export production.

Chapter 3 brings the story back to Fe with a look at evidence for Fe-limitation further north in the California Current System than previously identified. The

southern California Current System has been shown to have an Fe-limitation mosaic (Hutchins et al., 1998) with many narrow shelf, low river input regions showing evidence for Fe-limitation (Biller et al., 2013; Bruland et al. 2001; Firme et al., 2003; Hutchins et al., 1998; King and Barbeau, 2007). Work further north in the California Current System, off of northern Oregon and Washington, has shown plentiful Fe as a result of the Columbia River and a wide continental shelf (Bruland et al., 2008). In Chapter 3, we study a location between these regions, off the coast of Cape Blanco in southern Oregon. We investigate Fe-limitation of coastal diatoms by both growth rate and biomass accumulation as in Biller et al. (2013), and find evidence that both are limited by Fe in this region. This evidence suggests that the Fe-limitation mosaic extends further north than was previously known, which could have implications for global models of primary productivity.

This dissertation expands on the knowledgebase of two elements in the ocean: Fe and Sc. Iron has been studied more than any other trace element in the ocean, and is an essential and often limiting micronutrient, yet the Fe cycle remains difficult to fully understand. Scandium has hardly been studied at all, yet work in this dissertation shows that it can be a useful tool for understanding processes in the ocean, potentially including the oceanic Fe cycle. Studying these two elements gives us new insights into physical, chemical, and biological processes occurring in the ocean.

References

Biller, D.V., T.H. Coale, R.C. Till, G.J. Smith, and K.W. Bruland (2013), Coastal iron and nitrate distributions during the spring and summer upwelling season in the central California Current upwelling regime, Cont. Shelf Res., 66, 58-72, doi: 10.1016/j.csr.2013.07.003.

Bruland, K. W., and Lohan, M. C. (2003), Controls of trace metals in seawater, Treatise on Geochemistry. Elsevier Ltd., V6, [ISBN: 0-08-044341-9], 23-47.

Bruland, K.W., E.L. Rue, and G.J. Smith (2001), Iron and macronutrients in California coastal upwelling regimes: implications for diatom blooms, Limnol. Oceanogr., 46, 1661–1674, doi: 10.4319/lo.2001.46.7.1661.

Bruland, K.W., M.C. Lohan, A.M. Aguilar-Islas, G.J. Smith, B. Sohst, and A. Baptista (2008), Factors influencing the chemistry of the near-field Columbia River plume: Nitrate, silicic acid, dissolved Fe, and dissolved Mn, J. Geophys. Res., C00B02, doi:10.1029/2007JC004702.

Bruland, K.W., R. Middag, and M.C. Lohan (2014), Controls of trace metals in seawater, Treatise on Geochemistry (2nd edition), Elsevier, Oxford, [ISBN: ISBN: 978-0-08-098300-4],19-51, doi:10.1016/B978-0-08-095975-7.00602-1.

Byrne, R. H. (2002), Inorganic speciation of dissolved elements in seawater: the influence of pH on concentration ratios, Geochem. Trans., 3(2), 11-16, doi:10.1039/b109732f.

Firme, G.F., E.L. Rue, D.A. Weeks, K.W. Bruland, and D.A. Hutchins (2003), Spatial and temporal variability in phytoplankton iron limitation along the California coast and consequences for Si, N, and C biogeochemistry, Global Biogeochem. Cycles, 17, 1016, doi:10.1029/2001GB001824.

Hutchins, D.A., G.R. Ditullio, Y. Zhang, and K.W. Bruland (1998), An iron limitation mosaic in the California upwelling regime, Limnol. Oceanogr., 43, 1037–1054, doi: 10.4319/lo.1998.43.6.1037.

King, A.L., and K. Barbeau (2007), Evidence for phytoplankton iron limitation in the southern California Current System, Mar. Ecol.-Prog. Ser., 342, 91–103, doi: 10.3354/meps342091.

Parker, C.E., M.T. Brown, and K.W. Bruland (accepted), Scandium in the open ocean: A comparison with other group 3 trivalent metals, Geophys. Res. Lett., doi:10.1002/2016GL067827.

Rogers, H.J., C. Synge, and V.E. Woods (1980), Antibacterial effect of scandium and indium complexes of enterochelin on Klebsiella pneumoniae, Antimicrob. Agents Ch., 18(1), 63-68, doi:10.1128/AAC.18.1.63.